Journal of Volcanology and Geothermal Research 364 (2018) 1–19

Contents lists available at ScienceDirect

Journal of Volcanology and Geothermal Research

journal homepage: www.elsevier.com/locate/jvolgeores

Linking lava flow morphology, water availability and rootless cone formation on the Younger Laxá Lava, NE Iceland

Frances Boreham [a,*], Katharine Cashman [a], Alison Rust [a], Ármann Höskuldsson [b]

[a] School of Earth Sciences, University of Bristol, Wills Memorial Building, Queens Road, Bristol BS8 1RJ, UK
[b] Institute of Earth Sciences, University of Iceland, Sturlugata 7, 101 Reykjavik, Iceland

ARTICLE INFO

Article history:
Received 17 May 2018
Received in revised form 20 August 2018
Accepted 25 August 2018
Available online 1 September 2018

Keywords:
Rootless cone
Pseudocrater
Hydrovolcanism
Lava–water interaction
Hornito

ABSTRACT

It is well established that rootless cones and associated deposits are the result of explosive interactions between lava flows and environmental water, but there is substantial uncertainty about the dynamics of rootless eruptions, particularly the relative importance of lava supply, water availability and the conditions under which they meet. Here we present a case study of the Younger Laxá Lava in NE Iceland, and the >6500 rootless cones that it created. Critically, this long (63 km) lava flow interacted with water along its length, from flow through/around a large lake (Mývatn), down a narrow river gorge (Laxárdalur) and across a broad glacial valley with wetlands and rivers (Aðaldalur). Using high-resolution digital terrain models and aerial photographs, we map the flow surface morphology, and classify, measure and analyse the rootless cone type, size and spatial distribution in the context of both lava and water availability. We find that rootless cone size is controlled by the combined availability of lava and water: large rootless cones require sustained, high volumes of lava (related to proximity to vent) and water (e.g., Lake Mývatn), whereas limited supplies of lava (with distance from the vent and from the centre of the flow) and water (particularly in dammed river valleys) build smaller cones. Where we infer that where water was distributed in sediment, the lava–water interaction style changed to low-energy and distributed bubble bursts that created >3000 hornitos in the lower reaches of Aðaldalur. The distribution of rootless cones around Mývatn also defines the pre-eruption extent of the lake and suggests substantial lake level changes during the course of the eruption. By looking at the variation in rootless cone type and size in the context of the parent lava flow and the local environment, we explain how the availability of water and local mass flow rate of lava affect the dynamics of rootless eruptions.

1. Introduction

Rootless eruptions are the result of explosive interactions between lava and external water. They are driven by steam generated as a lava flow heats trapped water or ice in the underlying sediment (e.g. Mattox and Mangan, 1997; Hamilton et al., 2010a) and are therefore common in environments where water is abundant, such as lakes, rivers, wetlands and coastal regions. Rootless cones and associated deposits are widespread across Iceland, Hawai'i, the Galapagos Islands and the Columbia River Flood Basalts (Thorarinsson, 1953; Mattox and Mangan, 1997; Jurado-Chichay et al., 1996; Reynolds et al., 2015; Ross et al., 2014). These locations share the characteristics of abundant (low viscosity) basaltic lava and plentiful surface water. For this reason, identification of rootless cone fields on Mars, with the implications for past surface water, has prompted studies of terrestrial cones as analogues (e.g. Fagents et al., 2002; Hamilton et al., 2011).

The association of rootless eruptions with otherwise relatively 'safe' lava flows makes them particularly dangerous for observers and tourists (e.g. Mattox, 1993). While there are numerous cones intact in Iceland and across the world, the only two witnessed events on inland lava flows left no trace or were destroyed by their parent lava flow (Fimmvörðuháls in 2010, Edwards et al., 2012; Mount Etna in 2016, e.g. Cummins, 2017), and littoral cones are rapidly eroded by waves (Jurado-Chichay et al., 1996). Therefore, it is likely that rootless eruptions are more common than the preserved deposits suggest. A better understanding of the conditions that lead to rootless eruptions can improve lava flow hazard assessments, shed light on past environmental conditions and increase our knowledge of broader interactions between magma or lava and water.

The dynamics of lava–water interactions (LWI), and the type of deposits produced, are affected by the lava flow properties, available water and the degree of mingling between the two (e.g. Fagents and Thordarson, 2007). However, there is still substantial uncertainty around the role of each variable and how they affect the morphology, deposit type (dominantly ash, scoria or spatter) and spacing of rootless cones. In this paper we examine the morphology of the Younger Laxá

* Corresponding author.
E-mail address: frances.boreham@bristol.ac.uk (F. Boreham).

https://doi.org/10.1016/j.jvolgeores.2018.08.019

Lava (YLL) in NE Iceland and the thousands of rootless cones it created as it flowed from its source east of Lake Mývatn, through the Laxárdalur gorge and into the glacial U-shaped valley of Aðaldalur (Fig. 1). We also present a detailed description and analysis of the cones in Laxárdalur and Aðaldalur. The YLL is a particularly good case study because it created a variety of rootless eruption features (scoria cones, spatter cones and hornitos) as it interacted with different water sources (lake, rivers, wetlands). Our goal is to link the lava emplacement style, its response to, and modification of, the local environment and available water, and the variation in size and type of rootless cones. This will allow us to better understand the factors that control rootless cone formation, interpret deposits on Earth and Mars, and inform hazard assessments for future lava flows in water-rich environments.

2. Background

2.1. Rootless cone formation

Rootless cones, so-called because they are not connected to a magma reservoir at depth and so have no geological 'roots', are created by explosive LWI and come in a range of sizes and types (Fagents and Thordarson, 2007). Rootless cones of ash, scoria and spatter range from metres to hundreds of metres in diameter (Fig. 2a); hollow spatter cones and small stacks of spatter (hornitos) can be only a few metres across (Fig. 2c–d).

Previous studies have linked cone morphology and pyroclast type (ash, scoria or spatter) to the conditions of cones formation. In Iceland, the ratio between crater radius and outer flank radius of larger cones resemble tuff rings, whereas smaller cones are steeper and similar to cinder cones, suggesting a link between morphology and formation conditions (Greeley and Fagents, 2001; Fagents et al., 2002). Fagents et al. (2002) compared the morphology and grain size of different cone groups in Iceland and found that larger cones tended to be made of vesicular, angular lapilli, whereas smaller cones tended to be more spatter-rich, implying weaker fragmentation. Similarly, studies of littoral cones (formed when lava flows reach the ocean) show that cones on flows fed by high lava fluxes tend to be larger and finer-grained than those where lava flux is lower. For example, littoral cones formed by high-flux 'a'ā flows can reach 450 m diameter and are typically composed of both coarse and fine ash (Moore and Ault, 1965; Fisher, 1968), whereas littoral cones on lower-flux pāhoehoe flows tend to be smaller (30–300 m diameter) and composed of lapilli and spatter clasts (Jurado-Chichay et al., 1996; Mattox and Mangan, 1997). The same dependence on flow rate is observed on the Nesjahraun lava flow at Þingvallavatn, a large lake in central Iceland (Fig. S1). As the lava entered the lake it produced two rootless cones: Eldborg formed on a pāhoehoe lobe, is 150 m in diameter and constructed of layers of scoria with a 3 m cap of spatter; Grámelur, a pair of half-cones on an 'a'ā flow lobe, is 400 m long and made of coarse ash and angular lapilli (Stevenson et al., 2012).

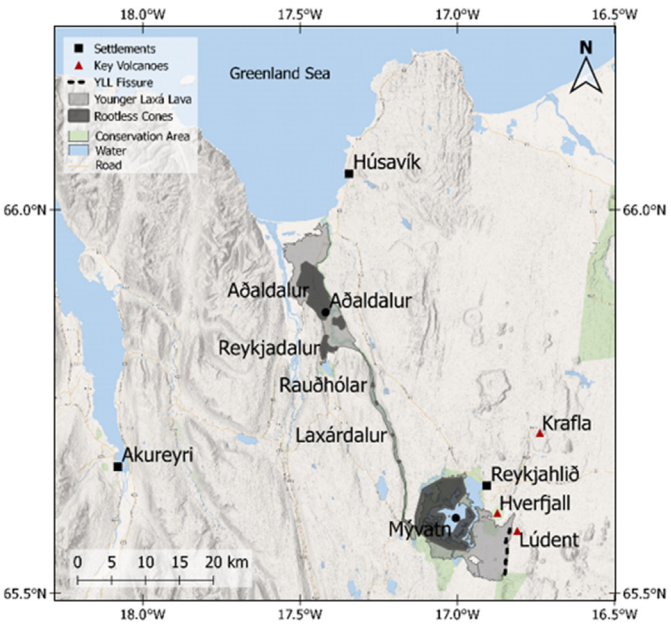

Fig. 1. View of the Mývatn, Laxárdalur and Aðaldalur region. The extent of the Younger Laxá Lava is shown in grey. Orange areas highlight the groups of rootless cones. Key local volcanic centres are shown by red triangles. Nearby settlements are shown with black squares. Green areas represent conservation areas or national parks.

The size, vesicularity and shape of pyroclasts depend on the fragmentation energy: small grain sizes require higher explosive energy than larger clasts and spatter (Sheridan and Wohletz, 1983; Zimanowski et al., 1997a; White and Valentine, 2016; Sumner et al., 2005). Therefore, the range in pyroclast types and sizes at rootless eruption sites, from very fine ash to welded spatter, shows that the dynamics of LWI can vary considerably. The finest ash in scoriaceous rootless cones (3.5–4 φ; 88–62 μm) is commonly attributed to a highly explosive form of steam eruption known as a fuel–coolant interaction (FCI; Hamilton et al., 2017, Fitch et al., 2017; Zimanowski et al., 1997b). Similar grain sizes are, however, produced when vesiculating magma interacts with water (Liu et al., 2015). In FCI, the grain size distribution is controlled by the kinetic energy release, which is controlled by the mass ratio of interacting lava and water (Sheridan and Wohletz, 1983). This depends on the contact surface area between lava and water over which heat transfer takes place, and a degree of mingling between the two fluids is generally required to reach sufficient heat transfer rates to initiate an explosion, either through hydrodynamic mingling or brittle fragmentation (Austin-Erickson et al., 2008; White and Valentine, 2016; Wohletz et al., 2013). It is important to note that the interacting lava–water mass ratio may be different from the total ratio of lava and water in the wider environment, and explosions can occur in apparently suboptimal conditions (White and Valentine, 2016). However, the bulk of the mass of rootless scoria cones is built of lava that was not active in FCI (Hamilton et al., 2017; Fitch et al., 2017). While only the finest particles are created at the 'active' lava-water interface in an FCI, the energy released by the explosion will also affect the fragmentation of other lava it passes through, thereby indirectly controlling the grain size distribution of the rest of the deposit, including fluidal, blocky and mossy morphologies that are comparable to those in Hawai'ian or Strombolian scoria cones (Walker and Croasdale, 1971; Hamilton et al., 2017). Rootless features formed predominantly or entirely of spatter (spatter cones and hornitos) are built through low-energy bubble bursts or the escape of pressurised lava and gas from a lava tube (Mattox and Mangan, 1997; Kauahikaua et al., 2003).

Rootless cone cross-sections reveal that deposits are often inversely graded with a cap of welded spatter (Thorarinsson, 1953; Fagents and Thordarson, 2007). They often contain layers, showing that large rootless edifices are built up over a series of repeated explosions at a single site, requiring a plentiful and continuous or pulsed supply of both lava and water to the eruption site (Hamilton et al., 2017; Fitch et al., 2017). The presence of armoured bombs (tephra covered in outer layers of lava) in rootless cones also demonstrates that cones are formed over a series of discrete explosions (Reynolds et al., 2015; Noguchi et al., 2016). Some rootless cones also have multiple inner craters, interpreted to have formed during a separate, later phase of cone building driven by a recharge in water supply (Noguchi et al., 2016). Here, the outer flanks are made of loose scoria and ash, with slopes limited by the angle of repose (~33°). In contrast, the inner cones often have a higher proportion of welded material and shallower slopes. Noguchi et al. (2016) also found that smaller scoriaceous cones with caps of welded spatter had higher slope angles at the summit than lower down the flanks, as spatter is not limited by angle of repose. These outer layers of welded spatter are common and have been linked to waning energy in the final stages

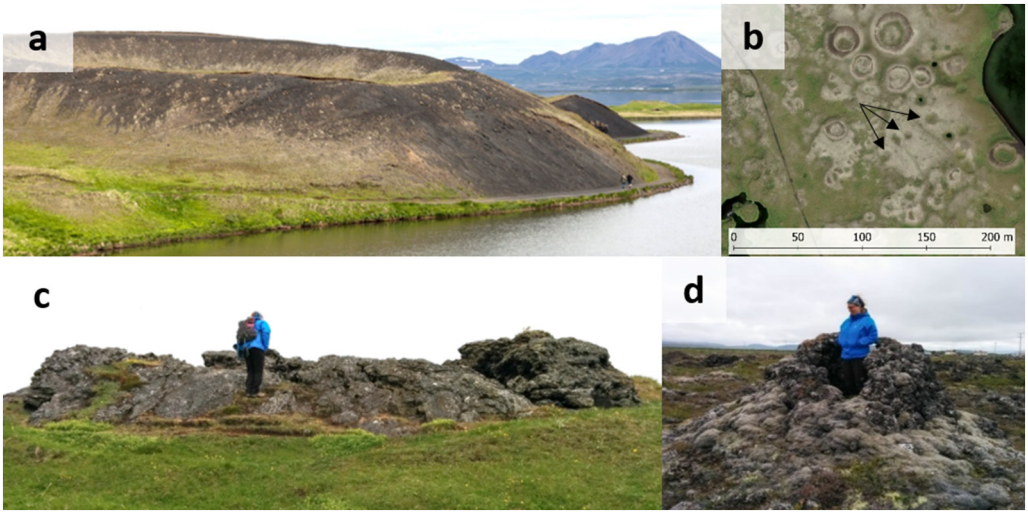

Fig. 2. Different types of rootless cone and associated features. **a)** Scoriaceous rootless cone at Skutustaðir, Mývatn. Cone base is ~100 m diameter. **b)** Explosion pits (marked with arrows) surrounding a scoriaceous rootless cone near Mývatn. **c)** Spatter cone at Mývatn. **d)** Hornito in Aðaldalur, NE Iceland. Map imagery on d ©2017 DigitalGlobe, Google.

of rootless eruptions as the availability of either lava or water dwindle (e.g. Fagents and Thordarson, 2007).

The approximately symmetric shape and often sizeable edifices of surviving rootless cones show that they form on lava flows with a solid top crust capable of supporting tephra deposits, as tephra falling on a moving flow would be swept away rather than building up a cone (e.g. Fagents and Thordarson, 2007). However, the weight of the resulting edifice can be enough to deform and crack crusts, leaving cones on tilted platforms (Jaeger et al., 2015; Keszthelyi et al., 2010). The substantially-crusted lava confines any water trapped below it in pools or sediment which aids the build-up of pressure as it is heated by the lava (Fagents et al., 2002). The formation of cones on established lava flows means that they are often associated with lava tube systems, and different cone morphologies are associated with tube, channelised and sheeted lava flows (Hamilton et al., 2010a). Clusters of cones may exhibit self-organisation, and active rootless eruption sites may be analogous to a series of hydraulic wells, drawing water from their surroundings (Hamilton et al., 2010b). In this scenario, the nearest neighbour (NN) distance is limited by the amount of water that each site can draw and the ease of water or steam transport to get to the eruption site.

These previous studies show that cone morphology and grain size distribution are affected by a range of factors. Where FCI takes place, the contact area and degree of mingling between lava and water control the interacting mass ratio of lava and water, which will in turn control the explosive energy released and therefore the grain size distribution of the deposit. However, the size and shape of the edifice will ultimately be controlled by the supplies of lava and water that sustain the eruption and build up the cone in layers. While past studies have looked at cone morphology, they have often been focussed on single sites; there has been no systematic quantitative comparison of rootless cones across different sites to examine the effect of lava and water supply rates on cone size, morphology and LWI dynamics.

2.2. Rootless cones in Iceland: Geological and hydrological setting

The combination of a wet climate and many basaltic eruptions means that Iceland has the most rootless cones on Earth: more than 13,000 cones and other rootless features created by least six eruptions (Fig. S1). Of these, the rootless cones around Mývatn, within the Northern Volcanic Zone (Fig. 1), are the most famous and most extensively studied in Iceland. Thorarinsson (1953) was the first to establish that they were caused by interactions between the YLL and lake water and were not primary craters. The numerous multiple-cratered cones surrounding Mývatn are suggested to have formed by successive discrete phases of explosive LWI, controlled by the supply of water to the site of the rootless eruption (Noguchi and Kurita, 2015; Noguchi et al., 2016). The Laxárdalur and Aðaldalur rootless cones were created by the same lava flow, although they have not been considered in detail by previous studies, and provide an opportunity to examine lava–water interactions along a far travelled lava flow through a variety of environments (lake, river valleys, wetlands).

Lake Mývatn lies ~50 km east of Akureyri, the largest city in northern Iceland (Fig. 1). It is a shallow eutrophic lake and Iceland's fourth-largest lake, ~10 km long and 7.5 km wide, covering an area of 37 km^2 (Einarsson et al., 2004). The northern edge of the lake, near the village of Reykjahlið, is marked by the end of the lava flow from the 1724–1729 eruption of Krafla, known as the Mývatn Fires (Einarsson, 1982). The basin of the pre-YLL lake Mývatn was formed by the Older Laxá Lava (OLL), which erupted ~3800 yBP from a shield volcano 25 km south of Mývatn (Einarsson, 1982). This lava flow underlies the YLL at Mývatn and through the Laxá gorge; drilling during the construction of a hydro-electric power station at the end of the gorge showed that the OLL was ~20 m thick, ~600 m from the start of Aðaldalur (Fig. 1; Thorarinsson, 1951). There are no known outcrops of the OLL in Aðaldalur. Early studies attributed the rootless cones in Aðaldalur to the OLL (Jakobsson, 1963), but they were later shown to be from the Younger Laxá Lava (YLL; Thorarinsson, 1979; Sæmundsson et al., 2012).

Present-day Mývatn was created by the YLL, which erupted from the Þrengslaborgir–Lúdentsborgir crater row 5 km to the east of Mývatn at 2180 ± 34 yBP (Fig. 3; Höskuldsson et al., 2010). The eruption produced 3.7 km^3 of lava with an average thickness of ~17 m and covered an area of 220 km^2, travelling 63 km from the fissure (Höskuldsson et al., 2010). To put it into perspective, this makes the YLL an order of magnitude larger than the 1984 Mauna Loa eruption in Hawai'i, and over twice the volume and nearly three times the area of the 2014 Holuhraun eruption from Bárðarbunga in Iceland (Cashman and Mangan, 2014; Pedersen et al., 2017). Between the fissure and lake lies the area known as Dimmuborgir (meaning 'dark castles'), a complex of lava pillars, collapse slabs and lava tubes that has been interpreted as the remains of a rootless shield complex that formed when the YLL ponded and drained in stages. Skelton et al. (2016) estimated that the ponding and release of lava at Dimmuborgir produced discharge rates of 0.7–7 m^3/s that were sustained over days to weeks through a network of drainage channels and provided a continuous supply of lava to the eastern shore of Mývatn. The landscape to the east of Mývatn is dominated by a phreatomagmatic tuff cone and associated deposits (Fig. 3b), formed by the Hverfjall Fires eruptive episode ~2500 yBP

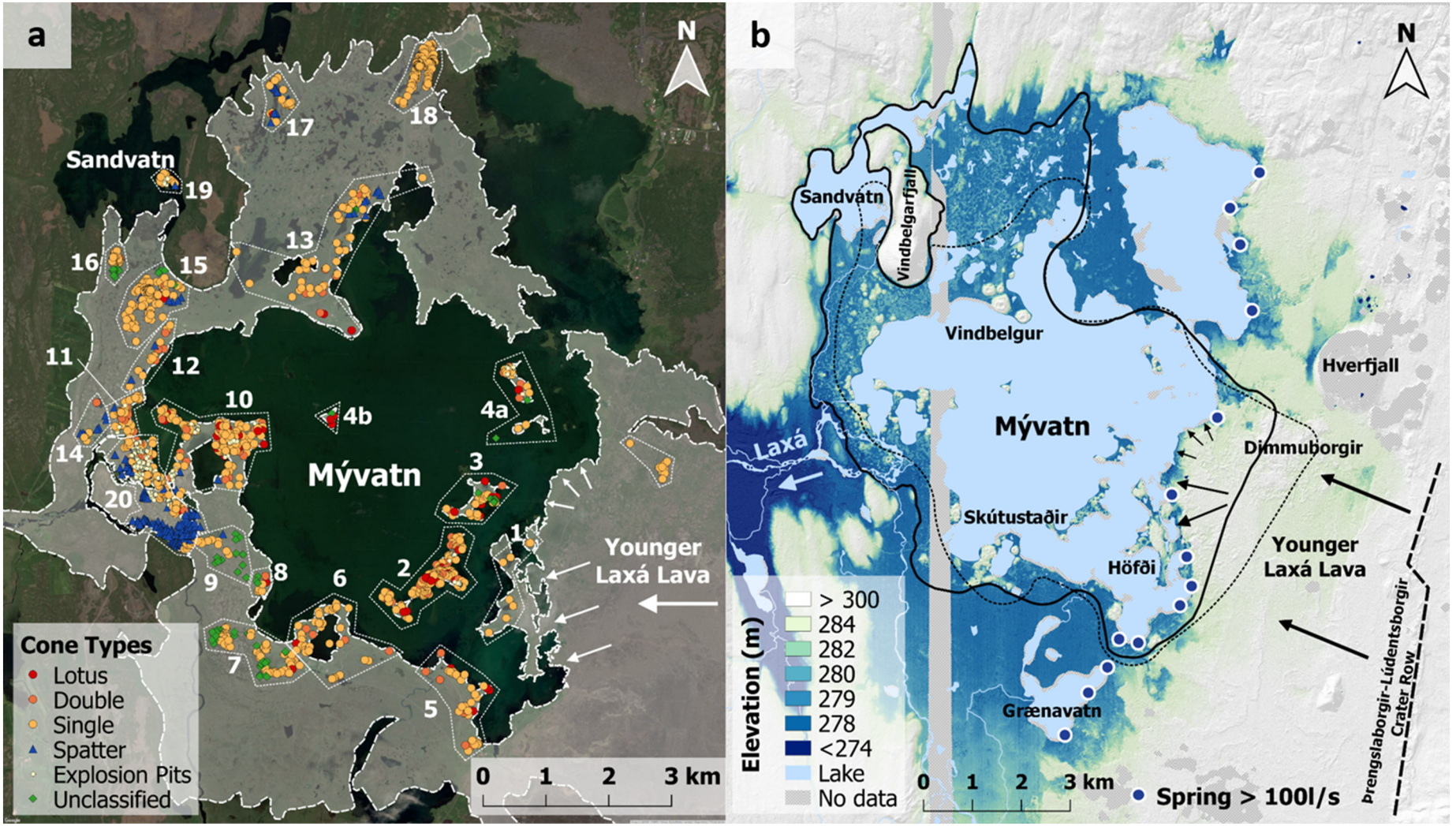

Fig. 3. a) Map of Mývatn showing the locations of rootless cones and extent of the Younger Laxá Lava, as mapped by Sæmundsson et al. (2012). Cone groups are outlined and numbered in a white broken line. Arrows show direction of lava flow and are sized to represent the volume of lava flowing in that area. Scoriaceous cones are marked as circles, spatter cones by triangles and unclassified cones as diamonds. **b)** ArcticDEM showing the elevation of the area around Mývatn, including the Younger Laxá Lava and surrounding countryside. Note that the colour ramp is scaled to highlight the area with an elevation of 279 m ± 1 m. The eruptive fissure is marked by the dashed black line, and arrows show the direction of the lava flow. Proposed outlines for the original lake are shown by a dotted black line (Einarsson, 1982) and solid black lined (this study). Major springs (> 100l/s) feeding Mývatn and Grænavatn are shown by blue circles. DEM created by the Polar Geospatial Center from DigitalGlobe, Inc. imagery. Map imagery ©2017 DigitalGlobe, CNES/Airbus. Map data ©2017 Google.

when a propagating dike encountered the active ground water system (Mattsson and Höskuldsson, 2011; Liu et al., 2017).

The YLL inundated and interacted explosively with an existing lake to create the famous Mývatn rootless cones (Thorarinsson, 1953). Analysis of the diatom layers shows that the lake took up to 700 years to recover and stabilise (Einarsson et al., 1988). Preserved diatoms in rootless cone tephra from around the lake show that it was originally larger and deeper than present day (Einarsson, 1982). Based on these diatoms and the rootless cone distribution, Einarsson (1982) proposed a minimum extent of the original lake that, in places, extends >1 km inland from the current lake shore. The ground around the cones and away from the lake is water-logged, with numerous small ponds, streams and wetland areas that make the region one of the Europe's largest breeding sites for water birds.

Today, the hydrological system in the region is dominated by Mývatn and the Laxá river, with smaller inputs from other rivers and streams. The cold and warm springs on the eastern shore of Mývatn provide a plentiful and steady supply of water to the lake at 32–33 m^3/s in

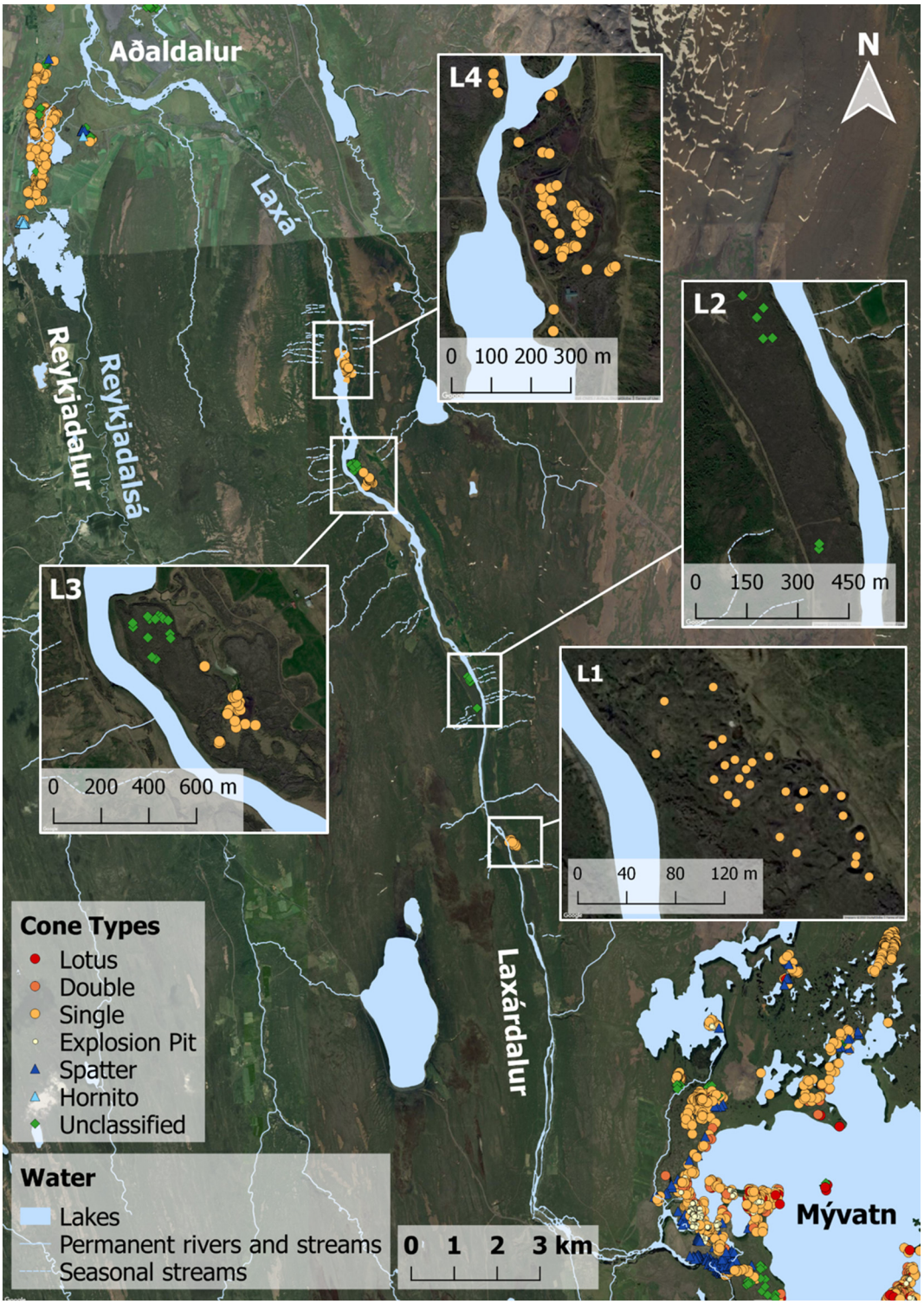

Fig. 4. Rootless cone groups along Laxárdalur, with inset close-up views of each group. Map imagery ©2017 DigitalGlobe, CNES/Airbus. Map data ©2017 Google.

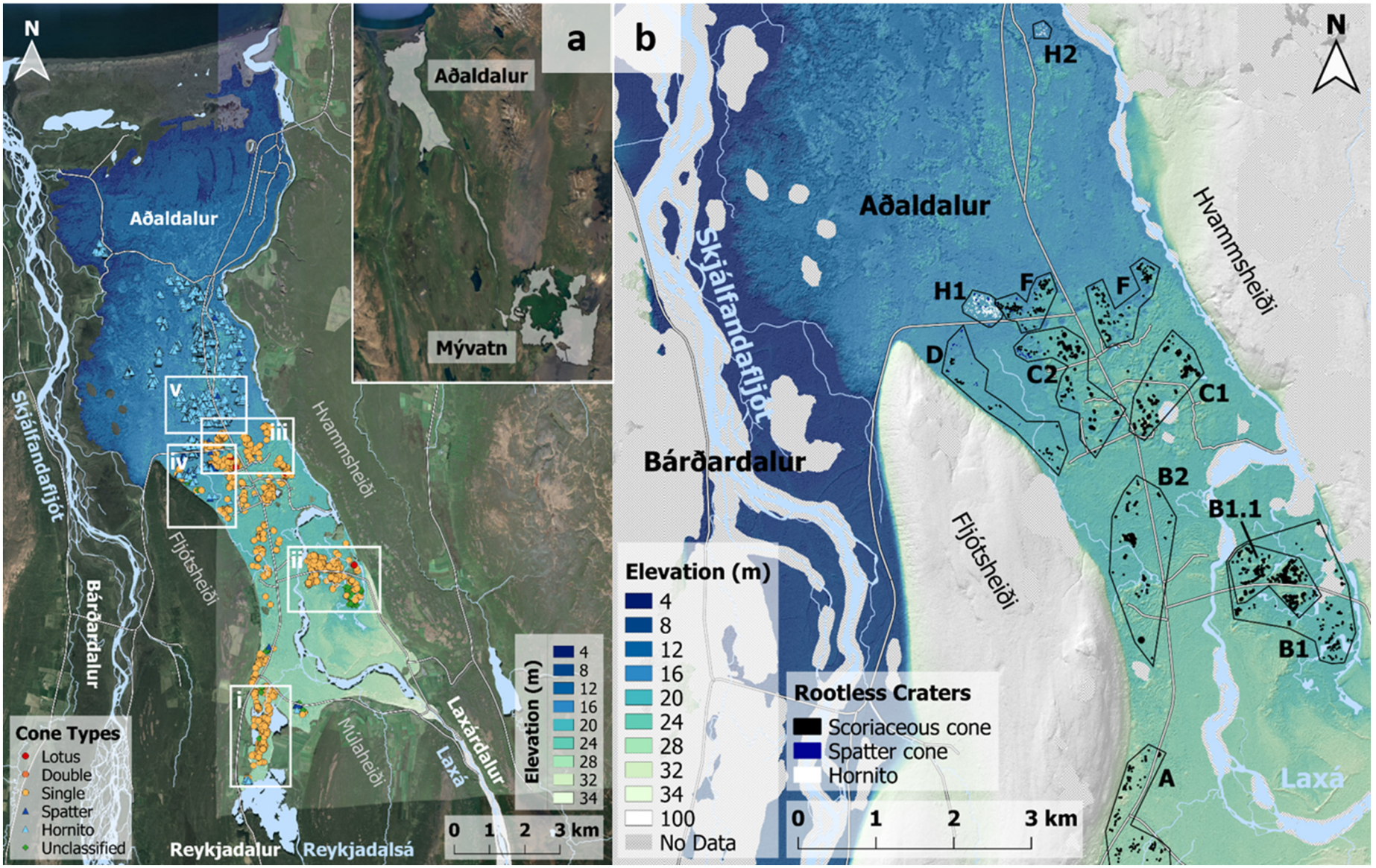

Fig. 5. The Younger Laxá Lava (YLL) in Aðaldalur and key geographical features. The elevation of the lava flow is taken from the 2 m resolution ArcticDEM dataset, clipped to the extent of the YLL in Aðaldalur. Principle rivers in the area are shown by pale blue lines and labelled in blue text. Valleys are labelled in black text and mountains and hills between valleys are labelled in grey. **a)** View of Aðaldalur showing the elevation of the lava flow and the location of rootless cones and hornitos. Scoriaceous cones are represented by circles, spatter cones and hornitos by triangles. White boxes **i–v** correspond to the views shown in Fig. 7 and Fig. S16. **Inset:** The extent of the YLL across Mývatn and Aðaldalur, with the site of the fissure eruption shown by a dashed line. The lava flow extent is based on the geological map of the area (Sæmundsson et al., 2012). **b)** View of the join between Aðaldalur and Bárðardalur, coloured by elevation. The craters of rootless cones and some hornitos in Aðaldalur are shown to highlight the change in cone size across the lava flow. Cones have been grouped by their location on the lava flow and correspond to the groups described in Results. Note that the holes and gaps in the DEM are gaps in the ArcticDEM dataset and are cross-hatched in grey. DEM created by the Polar Geospatial Center from DigitalGlobe, Inc. imagery. Map imagery ©2017 DigitalGlobe, CNES/Airbus. Map data ©2017 Google.

total, 44% of which comes from the springs near Höfði (Einarsson et al., 2004; Fig. 3). This inflow is balanced by outflow to the Laxá, which drains from the south-west corner of the lake and then flows north through the narrow Laxá gorge (Laxárdalur; Fig. 4) and the glacial U-shaped valley of Aðaldalur (Fig. 5) before draining into the Greenland Sea. As it flows through Laxárdalur, the Laxá is fed by small drainage streams off the surrounding highlands, which fluctuate seasonally with snowmelt (Fig. 4).

Laxárdalur opens into a flat plain, where it merges with the Reykjadalur valley to the west (Fig. 5). The Reykjadalsá river is substantially smaller than the Laxá because it drains the highlands west of Mývatn where there is a lower groundwater flow (Einarsson et al., 2004). Just before it joins the Laxá, the Reykjadalsá moves through an area of small lakes and wetlands. Similar but smaller ponds, providing contained but limited sources of water, are found throughout Aðaldalur. Half-way down, Aðaldalur merges with the adjacent valley of Bárðardalur, to the west. The river Skjálfandafljót, fed through Bárðardalur and travelling along the western side of Aðaldalur, is a shallow braided river with numerous banks and islands, and a bed > 800 m wide. Here, the Laxá is confined to the eastern edge of the valley by the YLL and is deeper and narrower (<100 m wide) than the Skjálfandafljót, confined to a single channel with only a few small islands. The northern end of the valley is covered by the YLL, where the lava surface is broken and heavily vegetated.

Lake Mývatn, the groundwater system feeding it and the Laxá and Reykjadalsá rivers all pre-date the YLL. The remains of birch trees immediately under the YLL in Aðaldalur and in the northern basin of Mývatn suggest that the climate at the time of the eruption was comparable to present-day (Hauptfleisch and Einarsson, 2012). The similar hydrology and climate mean that the range of environments and water sources in the region today are likely to be very similar to those encountered by the YLL.

3. Methods

3.1. Rootless cone types

We have divided the rootless cones in the study area into seven classes based on size, shape and pyroclast type (i.e. ash, scoria or spatter): single-cratered scoriaceous rootless cones (S; Fig. 2a), double-cratered scoriaceous cones (D), multi-cratered or 'lotus-fruit' cones (L), spatter cones (SP; Fig. 2c), hornitos (H; Fig. 2d) and explosion pits (P; Fig. 2b). These classifications are consistent with previous studies of rootless deposits. Any cones we were not able to categorise with certainty are referred to as 'unclassified' (U).

Scoriaceous rootless cones are the most common and widely distributed cone type and include three different classes based on the number of summit craters (inner cones) present. The classic rootless cone is a low-profile single-cratered (S) cone composed of scoria and ash, often with a layer of welded spatter covering the top surface (Thorarinsson, 1953; Fagents and Thordarson, 2007). Rootless cones may have multiple craters at their centre, positioned above a 'rootless conduit' filled with denser, welded material. Cones with two craters (i.e. an inner cone inside an outer cone), often concentric, are referred to as double cones (D). Outer cones with more than one inner cone have been called 'lotus-fruit' scoriaceous cones (L; Noguchi et al., 2016). The basal diameters of scoriaceous rootless cones found in this study range from metres to hundreds of metres, with the largest single cones ~200 m diameter, and multi-cratered cones up to 350 m diameter.

Spatter cones were first described by Thorarinsson (1953) as *schweiss-schlacken* cones, meaning 'welding slag'. They are made entirely from agglutinated spatter, with no ash or loose scoria (Fig. 2c). The spatter cones in this study are hollow with sloping walls and have basal diameters of 5–50 m. Spatter cones tend to have steeper slopes than scoriaceous cones, as their construction is not limited by angles of repose and they are more resistant to erosion (Thorarinsson, 1953).

Hornitos, meaning 'little ovens', are stacks of welded spatter a few metres in diameter and height, and are often hollow (Fig. 2d). We distinguish hornitos from spatter cones by size and aspect ratio: they have diameters ≤ 5 m and a height comparable to or greater than the diameter. Large fields of hornitos have been reported where lava flows encountered a shallow lake in Wudalianchi National Park, China (Gao et al., 2013), and they are seen in close association with rootless cones in Aðaldalur. However, hornitos are not always a result of LWI and are often found above skylights in lava tubes where internal pressure causes lava to spatter and build up ramparts (Kauahikaua et al., 2003).

Explosion pits are rootless craters that have no built-up walls or ramparts (Fig. 2b). They are generally found clustered around a larger scoriaceous rootless cone and were probably sites of smaller or shorter-lived rootless eruptions whose cone walls have been buried by scoria from larger nearby rootless vents.

3.2. Aerial imagery and high-resolution DTMs from drone surveying

We use a combination of satellite and aerial photographs and digital terrain models (DTMs) derived from them. We primarily use Google Earth images from the DigitalGlobe image library, which have spatial resolutions of 0.35–0.58 m/pixel (see Table S1 for further details). Where the resolution of the Google Earth images was poor or where features were indistinct we referred to higher resolution Loftmyndir ehf. imagery available on http://map.is/base/m, which has a spatial resolution of 0.15–1 m/pixel (Loftmyndir, 2014; Noguchi et al., 2016). We supplemented these with high-resolution DTMs that we created using a small unmanned aerial system (UAS). We surveyed three rootless cone groups: (1) part of the first group of scoriaceous rootless cones in Aðaldalur (Fig. S2); (2) the transition from scoriaceous rootless cones to hornitos approximately half way down Aðaldalur (Fig. S3); and (3) an area of hornitos at the northern end of the valley (Fig. S4). We did not survey any areas around Mývatn because of the high density of nesting water birds.

To create our high-resolution DTMs, we used a DJI Phantom 2 Vision + quadcopter, which has an integrated camera. The battery life of quadcopters limits flight to approximately 15 min, enough to survey ~0.12 km^2. This limit made it unfeasible to cover entire cone groups, so we selected representative accessible areas within each group, or regions that contained features of particular interest. Flights were made in a regular grid pattern, controlled using the DJI Vision smartphone app. The grid spacing and altitude were chosen to give an overlap of >70% between adjacent passes and a spatial resolution of ≤10.5 cm/pixel (details flight time, altitude, grid spacing and spatial resolution of captured images of each flight are available in Table S2).

The on-board camera captured video at 1080p and 29 frames per second (fps) and 110° field of view, which was split into full size (1920 × 1080 pixel) JPEG images at a rate of 1 fps. This gave a minimum overlap of 80% between images in the direction of travel, ensuring good coverage when constructing a 3D model of the site. The images were processed and stitched together using Agisoft Photoscan, a commercial structure-from-motion software package. Because we chose to capture video, no GPS data were saved from the UAS, so we georeferenced our models in the Geographic Information Systems (GIS) package QGIS to features visible in the Google Earth base map. With these control points, we optimised and georeferenced the 3D models in Photoscan to produce fully georeferenced DTMs (see Table S2 for RMS errors on georeferencing). All elevations in the DTMs are relative and do not correspond to the altitude above sea level. The DTMs were exported from Photoscan as .tiff files (available in Supplementary Material), which were then imported into QGIS for further analysis.

To investigate the lava flow morphology, we also used the ArcticDEM dataset produced by the Polar Geospatial Center (available from the ArcticDEM webtool at: http://arcticdemapp.s3-website-us-west-2.amazonaws.com/explorer/), which provides 2 m/pixel DTMs across the arctic circle. DTMs are built from data gathered from

WorldView-1, WorldView-2 and WorldView-3 satellites and processed according to Noh and Howat (2015). Data are provided in swathes, which do not always overlap and sometimes have a vertical offset relative to adjacent swathes. Elevation is also provided as ellipsoidal height rather than orthometric height (m a.s.l.), and these factors must be corrected before using the data. The difference between orthometric and ellipsoidal height at a given point is displayed in the ArctiDEM wetbtool. The ArcticDEM coverage of both Mývatn and Aðaldalur are slightly patchy and there are some holes in the DTM (visible in Fig. 3, Fig. 5).

Mývatn is covered by two different swathes of data, separated by a gap, but no vertical offset. Using QGIS, we applied a −66.25 m correction to the Mývatn DTM to convert from ellipsoidal height to orthometric height. Aðaldalur also lies on the boundary between two overlapping swathes, which have a slight vertical offset from one another. We applied a vertical transform of +2.4 m to the western segment to bring it in line with the eastern segment and merged the two parts into a single DTM. A further correction of −68.4 m was applied to the merged dataset to convert the elevation to orthometric height. Finally, we cropped the DTM in Aðaldalur to the extent of the YLL, based on a geological map of the area (Sæmundsson et al., 2012).

3.3. Cone digitisation, classification, crater size and nearest neighbour analysis

To explore their distribution, we digitised rootless cones using QGIS, with Google Earth imagery as a base map. We digitised each cone as a point at the centre of the crater, or the inferred centre if the cone was incomplete, using the highest resolution image available for the area. Each cone was given a unique identifier combining its locality (Mývatn, Laxárdalur or Aðaldalur), a number and, in some cases, a sub-group number (e.g. *Ada2_1* for cone 1 in sub-group 2 in Aðaldalur).

Based on the images and field observations, we grouped the cones into previously listed categories (L, D, S, SP, H, P and U). Where adjacent cones overlap, we counted each crater as an S cone if the cone flanks were distinct. Multi-cratered cones (L and D) are distinguished from overlapping S cones by the presence of a single continuous, smooth exterior wall, although complex cone morphologies can make this distinction difficult (see Fig. S5 for example).

To improve cone classification, we compared field notes and photographs to the appearance of the different cone types in aerial photographs and the maximum slope angles in the high resolution DTMs. Among the Aðaldalur cones, S cones had slope angles of <20°. In contrast, SP cones had maximum slope angles > 25°, and were especially steep around the crater rim as a result of their hollow structure (Fig. S3). The steep crater edges help to identify SP cones in aerial photographs, especially in strong sunlight, as they cast a darker, sharper shadow than the gentler crater rims of S cones. Field observations and high-resolution slope maps show that hornitos also have high (>30°) maximum slope angles (Fig. S3). Two other differences between S and SP cones are that: (1) all of the S cones in Aðaldalur showed some degree of oxidisation, giving the cones a reddish appearance in contrast to the grey SP cones; (2) many of the S rootless cones are vegetated, whereas the SP cones and hornitos host much less vegetation on their flanks. These qualitative data helped to distinguish between S and SP cones in the less accessible areas of the valley.

Not all of the digitised rootless cones have been classified because the aerial imagery was insufficient to distinguish cone type without additional field observations. The unclassified cones are all either small S cones or large SP cones because these two types are particularly difficult to distinguish. They make up 5.7% of the total possible population of S and SP cones, and 2.0% of all rootless cones.

To investigate variations in cone size, we digitised the craters of the rootless cones around Mývatn, in Laxárdalur and in Aðaldalur, using the Google Earth base-map, our high-resolution DTMs and the 2 m/pixel ArcticDEM data. Since hornito craters are too small to see in Google Earth images, we only digitised the craters of two groups of covered by our high-resolution DTMs. We used the radius of the crater rather than the whole cone as a measure of cone size because many cones have gentle slopes that overlap with adjacent cones, making it difficult to determine their extent. We approximated craters as ellipsoids in QGIS and calculated their areas using the QGIS field calculator.

We also categorised rootless cones based on their locality. Cone groups around Mývatn were initially given one of four classifications according to their proximity to the lake edge: islands (Is); lake shore (Sh); inland (In); at the mouth of the Laxá river (RM). The Laxárdalur cones form discrete groups, which we numbered 1–4 (Fig. 4). The cones in Aðaldalur were classified as: Reykjadalur (group A); ropy pāhoehoe (groups B1 and B2); inflated pāhoehoe (groups C1 and C2); the western edge of Aðaldalur (group D); along the inflation front (group F); and hornitos (groups H1 and H2; Fig. 5b).

We exported the locality, type, crater area, group and unique ID for each cone as a comma separated variable (.csv) file for further spatial analysis in statistical software package *R* (script available in Supplementary Material). To assess their spatial distribution, we used the *geosphere* package in *R* to calculate the distance in metres between each cone and the closest adjacent cone (i.e. the NN distance). Since the craters are ellipsoids, we calculated the radius of the circle of equivalent area for each crater to give a measure of cone size.

The number of digitised cones is a minimum estimate, as some rootless cones across the YLL have been quarried or demolished, and others may not be identifiable in existing aerial photographs (particularly small hornitos). The land around Mývatn and between the rootless cone groups has been farmed since the area was settled in the 10th Century AD. The cones at Mývatn are now protected, but we cannot rule out destruction by human activity in the past. The Rauðhólar cone group in Laxárdalur has been partially quarried. Some cones in Aðaldalur have clearly been demolished to make space for roads and buildings or excavated to improve farmland, and it is possible that more cones have been removed as a result of farming or development. Historical satellite images in Google Earth do not date back far enough to see the area before it was ploughed, but vegetation patterns in some fields hint at possible additional rootless cone sites.

3.4. Error analysis

Digitising cones and craters from aerial photographs introduces unavoidable uncertainty to the data set, as it requires judgement of the positions of the cone centre and crater edge. These errors are exacerbated by approximating the craters as ellipses. To assess the accuracy of our measurements of cone area and NN distance, we selected a sample of 315 cones in Aðaldalur and independently digitised the craters and cone centres four times (Fig. S6). We measured the crater area and NN distance for each repeat and amalgamated the datasets so that each cone had four associated values of area and NN distance. We then calculated the mean values for each cone, and the difference between the mean and each measurement to give a distribution of the absolute errors associated with crater area and NN distance. From the absolute errors and the mean, we calculated the relative errors and fit these to two Gaussian distributions in *R* (script in Supplementary Material; Fig. S7). We took the standard deviation of the fitted distributions as the standard errors for our area and NN measurements. We then converted the standard error of the area to an error for equivalent crater radius, to fit with our statistical modelling. We calculated a standard error of ±26.2% on crater area, corresponding to +12.3% / −14.1% error in equivalent radius, and a ±5.0% error on NN distance. This error is small enough that it does not affect the outcomes of the statistical modelling of different cone populations.

3.5. Statistical modelling

To explore the relationship between the size, type and NN spacing of the rootless cones, we carried out Analysis of Variance (ANOVA) tests on

the different rootless cone populations using the statistical package *R*. A base 10 logarithmic transform was applied to the radius and NN data to make the distribution appropriate for statistical modelling. All models were validated in *R* by checking that the assumptions of normally-distributed variables and heteroscedasticity were true, and that the model was not influenced by outliers. Each cone appears only once in the dataset, so there is no auto-correlation. A list of the ANOVA models and the dependent and independent variables for each is given in Table 1. Tukey Honest Significant Difference (HSD) tests were used to compare the means and give the significance between each explanatory factor (Table S3 in Supplementary Material). In line with standard practice, we took $p < 0.05$ as the threshold for determining statistical significance. The p-values are reported in Table 1 alongside the degrees of freedom and F-statistic, which gives a measure of the variability between groups compared to the variability within each group, for each model. We used the Akaike information criterion (AIC) to compare the quality of fit of the different models to the data: a lower AIC value indicates a better model fit.

We assessed the correlation between the size (crater radius) and NN distribution using a simple linear regression. We calculated the correlation coefficient (r) and corresponding p-value for the entire population, and for each locality (Mývatn, Laxárdalur and Aðaldalur) and type separately (Table S4). We then assessed difference in the size distributions of the different cone types (L, D, S, SP, H and P) across the whole YLL. We controlled for cone type in all subsequent models, unless otherwise stated. The quartiles, mean and standard deviation of NN distances for each group are given in Table 2.

We used a chi-squared test to compare the proportion of different cone types between the three sites: Mývatn, Laxárdalur and Aðaldalur. For this comparison, we used the whole population of hornitos in Aðaldalur, not just those with digitised areas. Because the number of cones at each locality varies by more than an order of magnitude, and not all cone types appear at each locality, p-values for the chi-squared test were calculated using a Monte Carlo test with 2000 replications to account for the fact that the count data for each type was not normally distributed.

We tested the relationship between cone size and proximity to the lake edge for the Mývatn cones using two different models: one where the cones were categorised based on their proximity to the current lake edge and one based on the proximity to the estimated edge of the lake before the YLL. We also tested to see whether there were any significant differences in cone size between the different Laxárdalur groups.

The distribution of rootless cones across Aðaldalur means that some groups contain only one type of cone, which violates the assumption of no collinearity in the independent variables necessary for ANOVA. To avoid this problem, we tested the relationship between cone size and type, and cone size and group, separately. We then tested the relationship between cone size and group for the S cones only. While this reduces the data available for analysis, S cones are the most numerous type across different lava flow textures in Aðaldalur and are also present at Mývatn and Laxárdalur, allowing comparison between the three localities. Hornitos are the most numerous cone by type in Aðaldalur, but we have size data for them in only two parts of the valley. Because the size of rootless cones is correlated to the NN distance, we did not model the NN distributions in terms of type and group separately.

3.6. Flow emplacement temperatures

To determine the change in lava temperature along the length of the YLL, we measured the glass composition of scoria samples from Mývatn and Aðaldalur (locations shown in Fig. S8). The Mývatn scoria clast was collected from the surface of one of the rootless cones at Skútustaðir (group 6 in Fig. 3a). The Aðaldalur sample came from an excavated rootless cone along the inflation front. Both samples were selected in the field for their high glass content. We have assumed that glassy material from rootless cone scoria records the temperature of the lava as it interacted with water, while recognising that this is a simplifying assumption and that lava flows are not homogenous in temperature.

We analysed thin sections of both samples on a JEOL JXA8530F Hyperprobe at the University of Bristol (20 keV accelerating voltage, 10 μm beam diameter, 5 nA current). We measured ten points per sample and normalised the proportion of each element or oxide based on the totals for each point. We took the mean value of the ten points to give the average glass composition for each sample. We then calculated the temperature of the melts when they were quenched from the weight % MgO, following the method of Putirka (2008).

4. Results

In this section we follow the path of the YLL from its eruptive vent near Lake Mývatn, through the Laxárdalur gorge and then along the

Table 1
List of statistical models used in this study.

	Model name	Dependent variable	Independent variables	Results (X^2, F, p)	Adjusted R^2	AIC	Data
X^2	–	Type	Location	$X^2 = 3795.4$[a] $p < 0.001$	N/A	N/A	All YLL cones and hornitos
ANOVA	AllModel1	Log_{10}(crater radius)	Location i.e. Mývatn, Laxárdalur or Aðaldalur	$F(2, 2866) = 114.8$ $p < 0.001$	0.07	2202	All YLL cones
	AllModel2	Log_{10}(crater radius)	Type i.e. L, D, S, SP, H P, U	$F(6,2862) = 376.3$ $p < 0.001$	0.44	762	
	AllModel3	Log_{10}(crater radius)	Location + Type	$F(8, 2860) = 317.8$ $p < 0.001$	0.47	610	
	MyvModel1	Log_{10}(crater radius)	Category (i.e. proximity to current lake edge) + Type	$F(8,1460) = 100.0$ $p < 0.001$	0.38	407	All Mývatn cones
	MyvModel2	Log_{10}(crater radius)	Modified category (i.e. predicted proximity to original lake edge) + Type	$F(8, 1465) = 108.0$ $p < 0.001$	0.40	330	
	LxModel1	Log_{10}(crater radius)	Group	$F(3, 106) = 2.2$ $p = 0.094$	0.032	−87.9	All Laxádalur cones
	AdaModel1	Log_{10}(crater radius)	Category i.e. grouping on YLL	$F(9, 1255) = 240.9$ $p < 0.001$	0.63	−113	All Aðaldalur cones
	AdaModel2	Log_{10}(crater radius)	Type	$F(5, 1260) = 286.5$ $p < 0.001$	0.53	187	
	AdaModel3	Log_{10}(crater radius)	Category	$F(6, 989) = 73.1$ $p < 0.001$	0.30	−125	S cones only in Aðaldalur
Linear model	AllModel5	Log_{10}(crater radius)	Log_{10}(NN) + Location + Type	$F(9, 2859) = 411$ $p < 0.001$	0.56	55	All YLL Cones

[a] Note: Monte Carlo simulation with 2000 replications was used because the size of samples at different locations differed by more than an order of magnitude.

Table 2
Size and nearest neighbour distribution for rootless cone groups in Mývatn, Aðaldalur and Laxárdalur.

	Group	Cat.	Modified cat.	n	Crater radius [m]							Nearest neighbour distance [m]						
					Min	Q1	Median	Mean	Q3	Max	Std. dev.	Min	Q1	Median	Mean	Q3	Max	Std. dev.
Mývatn	1	Sh	Sh	8	5.5	6.2	10.9	13.9	19.9	28.4	9.1	21.39	93.66	130.9	143.1	163.4	357.1	108.8
	2	Is	Is	128	0.9	4.2	6.8	9.492	12.3	44.6	7.4	4.8	19.1	27.0	29.7	38.7	97.4	14.5
	3	Is	Is	29	2.0	3.6	7.1	9.783	14.1	31.1	7.6	8.4	36.6	41.2	53.0	60.0	215.2	46.3
	4	Is	Is	35	1.4	3.0	5.2	9.386	10.7	41.6	10.4	5.0	13.6	34.8	54.9	75.8	385.1	69.2
	5	Sh	Sh	35	2.5	8.2	12.4	15.14	21.7	38.5	10.1	19.4	46.3	54.3	73.6	81.8	288.6	60.4
	6	Sh	Sh	39	1.6	4.3	6.9	12.19	17.9	39.0	10.6	15.8	31.6	46.1	69.6	91.4	361.7	66.2
	7	Sh/In	Sh/In-1	88	1.1	3.3	5.3	6.971	9.5	30.2	5.5	9.6	20.5	28.9	33.4	43.5	103.8	18.0
	8	Sh	Sh	10	3.2	6.1	12.4	20.12	19.1	64.4	21.0	21.7	35.4	41.4	50.0	64.8	100.0	24.9
	9	In	In-1	22	1.2	3.1	5.6	6.696	8.0	19.6	5.0	29.9	46.6	66.3	76.5	109.1	164.2	40.2
	10	Sh	Sh	218	1.1	3.1	6.1	8.641	13.0	36.3	7.2	3.3	16.5	26.0	30.5	37.5	141.3	22.4
	11	Sh	Sh	36	1.4	3.2	6.8	8.265	10.4	28.6	6.9	8.2	24.3	37.8	40.8	52.5	89.3	23.7
	12	Sh	Sh	18	1.9	4.7	8.7	11.07	13.0	32.2	8.8	19.4	42.7	60.0	64.3	88.1	112.3	32.0
	13	Sh	Sh	71	1.3	4.0	7.4	12.02	13.0	62.3	13.5	16.3	27.1	40.7	81.0	77.5	721.8	128.6
	14	In	In-1	12	3.9	5.3	11.4	12.07	15.7	28.5	7.9	21.9	32.0	37.3	58.6	66.1	250.7	62.8
	15	In	In-1	109	1.3	3.5	6.1	6.967	6.6	20.2	4.2	5.4	12.9	27.1	34.1	47.8	207.1	30.7
	16	In	In-1	49	1.8	2.7	3.6	4.215	4.7	13.8	2.5	8.2	12.0	14.1	16.8	17.7	42.1	7.8
	17	In	In-2	32	1.9	4.0	5.8	7.49	10.3	22.5	4.7	11.3	19.6	25.7	31.0	35.3	102.3	19.5
	18	In	In-2	155	1.1	2.7	3.7	4.112	4.8	18.6	2.3	3.3	8.4	11.4	14.9	17.1	94.0	11.9
	19	Is	Is	26	4.2	6.2	7.8	8.607	10.0	22.2	3.7	13.5	18.9	24.5	24.2	29.5	34.4	6.5
	20	RM	RM	363	0.9	2.1	3.4	4.672	6.0	38.5	3.9	4.3	10.3	19.7	23.7	30	182.3	18.5
	21	In	N/A	10	9.5	17.6	19.3	19.6	23.5	28.8	5.7	37.8	38.9	44.5	105.0	53.1	604.9	176.5
Laxárdalur	Lx1			27	1.8	2.7	3.3	3.6	4.0	7.7	1.5	6.5	9.2	13.6	15.4	15.8	43.5	10.3
	Lx2			7	1.8	2.6	3.0	2.9	3.4	3.6	0.7	15.4	21.4	27.5	32.3	34.4	71.4	19.0
	Lx3			33	1.1	2.4	3.1	3.1	3.4	9.5	1.4	6.5	11.3	14.5	23.2	19.8	175.2	30.4
	Lx4			43	1.6	2.6	3.4	3.8	4.8	7.3	1.4	5.4	8.2	13.9	18.1	20.7	64.5	14.2
Aðaldalur	A			225	1.3	2.9	4.0	4.6	5.8	23.9	2.8	5.5	15.3	22.7	28.4	33.2	187.2	22.9
	B1			308	1.4	3.7	5.7	6.3	8.4	19.1	3.2	6.1	13.4	17.9	22.4	23.4	200.8	18.9
	B2			64	2.0	4.8	6.1	7.7	7.9	33.9	5.8	7.6	13.4	22.2	37.6	38.2	264.7	49.7
	C1			74	2.6	6.5	8.8	9.8	12.6	30.2	4.9	9.1	18.3	23.7	32.6	44.7	100.5	20.7
	C2			114	1.1	2.8	4.9	6.1	7.5	23.2	4.8	5.3	17.0	23.7	36.6	39.3	263.5	42.6
	D			29	1.3	2.2	2.5	2.4	2.7	3.8	0.6	5.5	9.0	10.6	14.0	18.0	45.4	8.6
	F			224	0.8	1.9	2.8	3.1	4.0	9.6	1.5	5.2	10.4	14.4	18.3	20.3	175.4	17.8
	Sp			56	0.9	1.6	2.3	2.8	3.5	6.4	1.4	6.4	12.1	16.8	23.0	23.2	166.3	23.5
	H1			134	0.2	0.5	0.7	0.8	1.1	2.3	0.4	3.7	5.9	7.9	10.0	10.1	100.3	10.4
	H2			28	0.3	0.5	0.6	0.8	1.0	3.0	0.5	2.8	5.9	10.9	13.6	17.8	54.3	11.5

length of the broad Aðaldalur valley, describing the changes in flow morphology and the rootless cones from our analysis of aerial photographs, the ArcticDEM and our own high resolution DTMs. We then examine the relationship between the size, type and spacing of the YLL rootless cones, and the systematic variation of cone size across the lava flow.

4.1. The Younger Laxá Lava and associated rootless cones

4.1.1. Mývatn

On the eastern edge of the Dimmuborgir complex is a cluster of nine single-cratered scoriaceous (S) cones (group 21 on Fig. 3a). These cones have a mean basal elevation of 303.2 m a.s.l., making them the highest group of cones on the YLL, 27 m higher than current lake level. Einarsson (1982) found buried rootless cones between Dimmuborgir and Mývatn and showed that vesicles in these cones contain diatoms from the pre-existing lake.

South of Dimmuborgir, the surface of the YLL is dominated by pressure ridges showing that the lava flowed towards the lake, draining through channels (Fig. S9a; Fig. S10). This region begins as a single, coherent flow ~ 800 m wide, before splitting into two separate flow lobes: the larger (northern) lobe fans out to 1.4 km wide; the smaller lobe turns to the southwest and is ~250 m wide where it meets the current edge of the lake. Where these two lava lobes meet the present-day lake near Höfði, there are lava structures with bathtub rings and lava pillars (Figs. S9b, S9c) that suggest ponding and LWI, respectively (e.g. Gregg et al., 2000; Gregg and Christle, 2013; Skelton et al., 2016). Curiously, there are very few rootless cones in this region (an exception is group 1 in Fig. 3a).

The land around Mývatn and the central lake basin is blanketed by tephra from the rootless cones, which obscures the lava flow surface. Around and between the rootless cone groups, the lake edges comprise black beaches of coarse scoria (Fig. S11a). Aerial photographs show that the shores of the islands are the same and reveal the remains of islands, and possibly rootless cones, that have been eroded to black sandbanks in the lake (Fig. S11b–c).

The islands in eastern Mývatn are covered in scoriaceous rootless cones (groups 2–4), with 149 cones on the largest island alone. Most are S cones, although there are numerous double-cratered (D) and lotus-fruit (L) cones. There are also a few explosion pits (P) close to or surrounding the larger cones. We have not found any spatter (SP) cones or hornitos on the islands.

The rootless cones around the southern and western shores of Mývatn are also a mix of S, L and D cones (groups 5–8, 11–13). The Skútustaðir cones (group 6) are the most accessible and are a popular tourist attraction. A radial transect through this group shows that the cones become smaller with distance from the current lake edge, decreasing in crater radius from 39.0 m to 1.6 m over ~500 m (Fig. S12a). The largest rootless cones around Mývatn are the Vindbelgur cones (group 13), with crater radii ≤62.8 m. As with the Skútustaðir group, the largest of these are L and D cones that sit on a peninsula jutting into Mývatn (Fig. S12b).

There are also numerous rootless cone groups inland of the present-day lake, among smaller pools of water and wetlands (groups 9, 14–18), and on an island in Sandvatn (group 19). Because of nesting birds, most of these cones are inaccessible during the summer months, so we mapped them based on aerial photographs. The most northerly cones (group 18) lie at the furthest edge of the YLL and > 1 km from the shore of the present-day lake. These S cones form a densely packed, elongate group on either side of the ring-road around the lake. The scoria in the visible outer layers of these cones appears larger and denser than the scoria that makes up the Skútustaðir cones (Fig. S13). Finally,

there is a concentration of rootless cones where the lake drains into the Laxá river (Fig. 3a). We have split the cones here into two groups. Those at the mouth of the Laxá (group 20) are predominantly SP cones and are the smallest around Mývatn. Those closer to the lake (group 10) are larger and are a mixture of L, D, S, SP and P cones.

4.1.2. Laxárdalur

After leaving Mývatn, the YLL followed the course of the Laxá. Our glass geochemistry data show that the lava cooled very little as it progressed through Laxárdalur, dropping only 10 °C over 45 km: from 1175.0 ± 3.1 °C at the southern shore of Mývatn to 1165.0 ± 1.7 °C at the inflation front mid-way down Aðaldalur (see Table 3, Fig. S14), in agreement with a previous study (Aebischer, 2018).

The YLL created four distinct rootless cones groups in Laxárdalur (Fig. 4). The first group (L1) lies 12 km down the valley and contains at least 27 cones clustered along the eastern edge of the lava flow and river. We have provisionally identified these as S cones, but the group may also contain some SP cones. The second group is 16 km down Laxárdalur and comprises 7 cones in the middle of the lava flow on the western side of the river (L2). The third group, comprising 33 cones in the middle of the lava flow, lies 21.5 km down Laxárdalur where the valley temporarily widens from ~0.5 km to ~1 km (L3). The final, and largest, rootless cone group lies 24 km from Mývatn and is made up of at least 43 S cones (L4). It is known locally as Rauðhólar, meaning 'red hills', due to the orange-red colour of the weathered scoria. There is no apparent size difference between cones in the Laxárdalur groups, although the number of cones in each group is too small for robust statistical analysis.

4.1.3. Aðaldalur

As the YLL left the confines of Laxárdalur it spread out, filling the 3.7 km width of Aðaldalur and backing up into the adjacent Reykjadalur, initially covering the entire width of the valley but narrowing to the south (up the valley; Fig. 6a). Approximately 250 rootless cones are spread along the lava flow in Reykjadalur, with crater radii of from 1.3–23.9 m, terminating in a group of ~34 hornitos at the end of the lava flow. These cones are currently surrounded by wetlands and small lakes.

In Aðaldalur proper, the first few kilometres of the lava flow have a ropy surface texture, with metre-scale folds visible in both the ArcticDEM and aerial photographs (Fig. 6b). Individual folds can often be traced for hundreds of metres and outline several broad lobes in the flow as it spread across the valley. There are no cones in this part of the flow. The first rootless cones (group B1 in Fig. 5b; Fig. 6b) lie in a topographic depression on the eastern margin where the lava flow has no visible surface texture. Most of these cones form a single compact group (group B1.1), bordered by streams and a small lake (Fig. S15). They are predominantly S cones with crater radii ranging from 1.7 m–19.1 m. They are closely spaced for their size and many of the cones overlap with their neighbours. The remaining cones in group B1 are smaller and more widely spread. The land around the central cone group is covered with ploughed fields, and the main road cuts straight through the central cone group. Therefore, it is possible that the central group and the outer cones were once part of a single continuous group.

A second group of cones, on the western side of the ropy pāhoehoe flow (group B2, Fig. 5b), comprises several smaller sub-groups, the smallest being an isolated pair of cones. Cones are closely spaced within each sub-group, and the outer walls of adjacent cones often overlap. These cones are also located in a low-lying part of the lava flow among pools of standing water. A chain of S and SP cones and hornitos is spread over 2 km along the western margin of the YLL next to Fljótsheiði (Fig. S16a, group D, Fig. 5b). Going north down the valley, the cones in this group change from predominantly S to a mix of S and SP cones. At the northern end, hornitos appear and eventually join up with groups C2 and H1 (Fig. 6c). The surface of the YLL in this region is featureless, both in the ArcticDEM and aerial photographs.

Approximately 6.5 km down Aðaldalur, the YLL morphology changes abruptly from ropy pāhoehoe to a flow surface marked by depressions several metres deep and wide, which is characteristic of inflated lava flows (Fig. 6c). We interpret the depressions as inflation pits, formed when the lava flowed around an obstacle and then inflated, leaving behind a pit in the surface of the flow (Hon et al., 1994; Self et al., 1998). The scoriaceous cones on this part of the YLL are among the largest in the valley (Fig. 6c); they are more widely separated than those further up the flow and do not form discrete clusters (groups C1 and C2 in Fig. 5b).

The inflated region of the YLL terminates in a 4–6 m step down in the flow surface height, level with the northern end of the Fljótsheiði mountain (Fig. 5b, Fig. 6c). Numerous small S cones are distributed along the up-flow (southern) side of this step (group F), bordered by clusters of SP cones that transition abruptly to hornitos on the down-flow side. The SP cones are similar in size to the small S cones along the step and are larger than the nearest hornitos (group H1). Notably, SP cones are almost entirely limited to this transitional region with the exception of a few isolated SP cones in group D and a cluster of eight SP cones at the edge of group A.

The YLL hosts ~3800 hornitos, separated into several large groups. The hornitos are too small to see in the ArcticDEM but our high-resolution DTM of the transition region confirms that all of the hornitos fall on the down-flow side of the step (Fig. S3), which is located where Aðaldalur joins the adjacent valley, Bárðardalur (Fig. 5). The largest group contains 1422 hornitos and covers ~1.18 km^2 (Fig. S16b), almost twice the area of the largest group of scoriaceous cones in Aðaldalur (group B1; ~0.66 km^2, 308 cones). This part of the flow also has a pitted texture, though much of the region is vegetated, obscuring the surface of the lava. Both aerial photographs and the ArcticDEM show a dried-up river bed (likely the former course of the Skjálfandafljót) that flowed up to and along the margin of the YLL. Small streams are still present around the edge of the lava flow. The surface of the lava in this region is broken up by pits and cracks (Fig. S16b).

The YLL stopped approximately 18 km down the valley. There are no obvious changes in the surface morphology between the inflation front at the end of the lava flow, and the edge of the lava flow does not correspond to any features in the landscape that might mark an older coast. From this evidence, the lava does not appear to have reached the sea during the eruption.

Table 3
Chemical composition (%) of rootless scoria samples from the Younger Laxá Lava at Mývatn and Aðaldalur.

	Mývatn		Aðaldalur	
	Mean	Standard deviation ($n = 10$)	Mean	Standard deviation (n = 10)
SiO_2	49.95	0.17	50.06	0.22
CaO	12.36	0.16	11.92	0.21
TiO_2	1.89	0.02	2.03	0.04
AL_2O_3	13.23	0.11	13.04	0.11
Na_2O	2.27	0.08	2.33	0.12
MgO	6.87	0.12	6.49	0.07
K_2O	0.21	0.01	0.22	0.01
FeO	12.75	0.12	13.46	0.08
Cl	0.01	0.00	0.01	0.01
MnO	0.22	0.02	0.23	0.01
P_2O_5	0.18	0.02	0.20	0.02
F	0.06	0.07	0.01	0.10
Temp (°C)	1175.0	3.11	1165.0	1.72

The Mývatn sample was taken from the surface of a rootless cone at Skútustaðir. The Aðaldalur sample was taken from a rootless cone along the inflation front half way down the valley. Temperature in °C at each location was calculated based on the MgO content after Putirka (2008).

4.2. Rootless cone size and spacing

Our statistical analysis is used to assess the variation in cone type, size and spacing within and between the different rootless cone sites

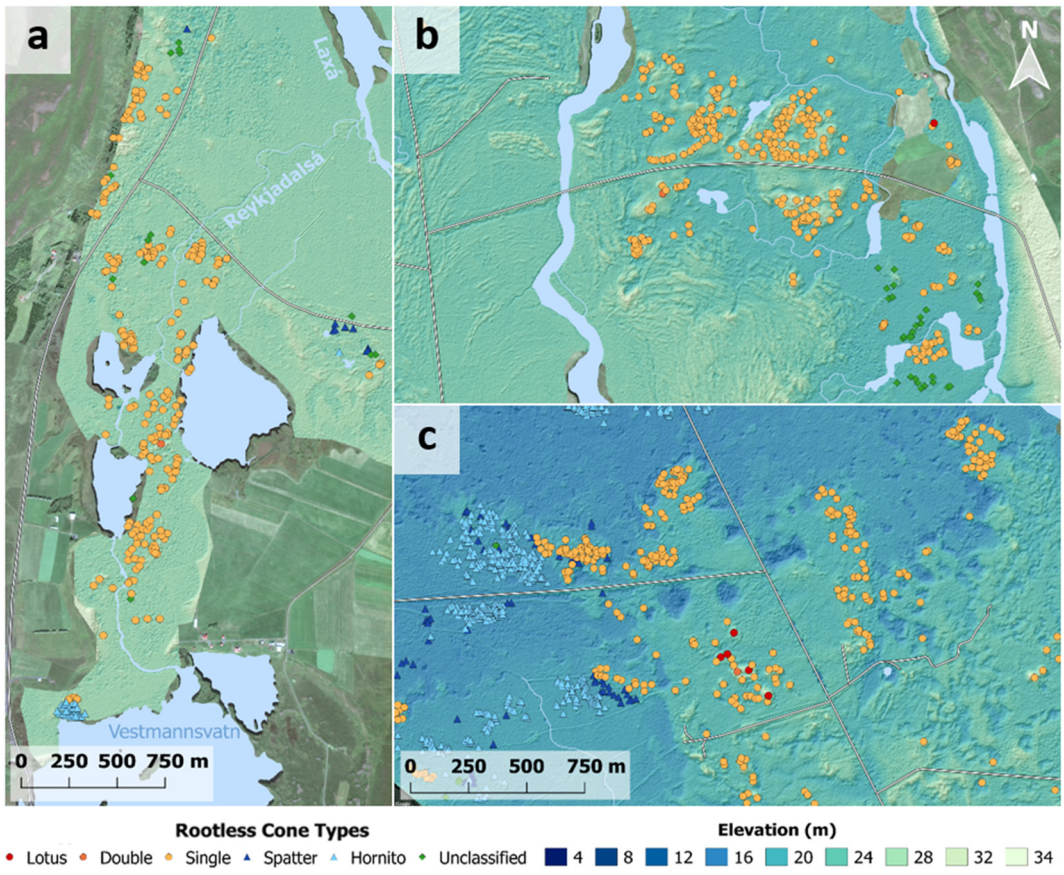

Fig. 6. Close-up of key regions of the Younger Laxá Lava, corresponding to areas **i–iii** marked in Fig. 5. **a)** Scoriaceous cones and hornitos formed when the YLL backed up into Reykjadalur and dammed the Reykjadalsá river. **b)** Scoriaceous rootless cones formed in a depression in the lava flow. The folds and wrinkles of ropey pahoehoe lava are visible in to the West of the cones. **c)** Pahoehoe lava flow marked with inflation pits. Scoriaceous rootless cones are found throughout this region of the lava flow and distributed along the inflation front. Hornitos and spatter cones are clustered downstream of the inflation front. DEM created by the Polar Geospatial Center from DigitalGlobe, Inc. imagery. Map imagery ©2017 CNES/Airbus, DigitalGlobe, Landsat/Copernicus. Map data ©2017 Google.

across the YLL. From our analysis of the lava flow morphology and water availability in the environment today, we link this variation to the inferred lava supply and water availability at the time of the eruption and variations in the LWI dynamics.

The different cone types are not equally distributed across the three localities (Table 4, Fig. 7a). Mývatn is dominated by scoriaceous cones with a high proportion of L and D cones (9.8%) but no hornitos. In contrast, Aðaldalur hosts ~3900 hornitos but far fewer L and D cones (0.22%). Cones in Laxárdalur show little variation and are all either S or unclassified (i.e. S or SP). Regardless of cone type, there is a moderate positive correlation ($r = 0.56$, $p < 2.2e\text{-}16$) between log crater radius and log NN distance (Figs. 8b, S17a), i.e. larger rootless cones tend to be further from their neighbours than smaller cones. Breaking the data down by locality shows that this correlation exists and is significant at both Mývatn ($r = 0.60$, $p < 2.2e\text{-}16$) and Aðaldalur ($r = 0.48$, $p < 2.2e\text{-}16$) but not in Laxárdalur ($r = 0.14$, $p = 0.16$; Fig. S17b–d). There is a significant correlation between crater radius and NN distance for all cone types except hornitos ($r_H = 0.14$, $p = 0.074$), ranging from weak to moderately-strong ($r_L = 0.38$, $r_D = 0.50$, $r_S = 0.45$, $r_{SP} = 0.40$, $r_P = 0.60$, $r_U = 0.49$; $p < 0.005$ for all these types; subscripts denote cone type; see Table S4 for 95% confidence intervals).

The size (crater radius) of rootless cones on the YLL varies with cone type, although not all cone types are distinct (Table 5; Fig. 7c). Specifically, there is no significant difference between the L and D cones. All other rootless cone types are significantly different in size from one another. L and D cones are on average larger than S cones ($M_L = 22$ m, $M_D = 17$ m, $M_S = 6$ m; M = mean, subscripts denote cone type), which in turn are larger than SP cones ($M_{SP} = 5$ m). Explosion pits are the next-smallest ($M_P = 3$ m), and hornitos are the smallest ($M_H = 1$ m). When comparing cones across all sites, unclassified cones and spatter cones are statistically indistinguishable ($M_U = 5$ m).

Rootless cone size varies with locality for all cone types (i.e. L, D, S and SP; Fig. 7d–f). The crater radius of cones around Mývatn is, on average, larger than cones in Aðaldalur (Table S3). There is no significant difference between the size of equivalent cones in Aðaldalur and Laxárdalur, but there are too few cones in Laxárdalur for a robust statistical test (Table S3).

Rootless cones around Mývatn decrease in size with distance from the lake edge (Fig. 8a). There is no significant size difference between cones on islands and those around the lake shore, although cones inland of the current lake shore are significantly smaller. The cones around the mouth of the Laxá river are the smallest. We note, however, that the extent of Mývatn was modified by the YLL, changing the distance between the cones and the lake. We divided the inland cones into two groups based on their proximity to the predicted lake before the eruption: groups 7, 9, 14–16 fall within the predicted lake (inland-1), and groups 17–18 fall on the predicted lake shore (inland-2). Comparing the crater radii of these two groups shows that they have statistically different size distributions. The inland-1 cone groups are similar to the shore and island cone groups (Fig. 8b). The inland-1 cones are smaller and closer in size to those at the river mouth, although the types of cones that make up the river mouth and inland-2 groups are very different: inland-2 is over 90% S cones, whereas the river mouth group has a more even mix of S, SP and P cones (Fig. S18).

In Aðaldalur, the crater size is affected by location on the lava flow (e.g. middle, margin or inflation front), both when considering all

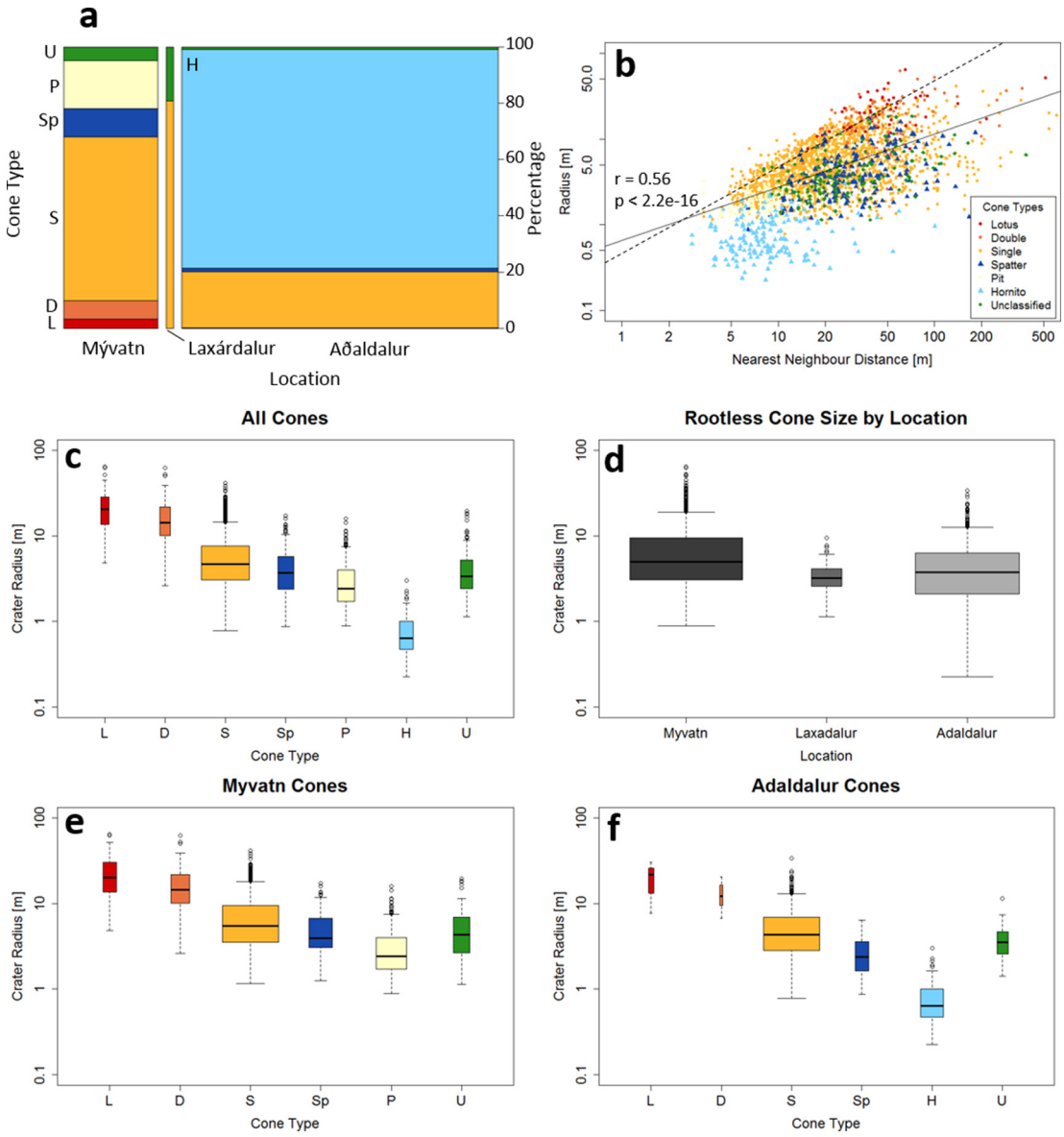

Fig. 7. Rootless cone properties across the Younger Laxá Lava, coloured by cone type. **a)** Scatter plot of crater radius and nearest neighbour distance for all YLL cones. Solid line shows the correlation between cone size and NN distance, with correlation coefficient (r) and p-value quoted. Dashed line shows the relationship y = (x/2) i.e. the NN distance is half the crater radius (i.e. points above this line represent overlapping cones). **b)** Distribution of the different types of rootless cones in Mývatn, Laxárdalur and Aðaldalur. Cones are coloured using the same scheme as other Figs. Bar width is proportional to the number of cones in the sample (see Table 5 for details). **c–f)** Variation in rootless cone crater size across the YLL, Mývatn, Laxárdalur and Aðaldalur respectively. Black circles represent data points that lie more than 1.5 times the inter-quartile range away from the median (outliers). Cones are coloured by type, consistent with the colour scheme used throughout this paper. Bar width is proportional to the number of cones in each sample (see Table 5 for details).

cone types, and when considering S cones only (Fig. 9, S17). Cones formed in the middle of the lava flow (groups B1, B2, C1 and C2) are larger than those at the margins of the flow or along the inflation front part-way down the valley (groups D and F). The cones in Reykjadalur (group A) fall between the size ranges of the ropy and inflated groups (B1, B2, C1, C2), and those on the flow margins (D and F).

Hornitos are the smallest rootless features in Aðaldalur and show very little variation in size across the valley (Fig. S19). The two groups measured (H1 and H2) have almost identical size distributions and though this represents only a small sample of the hornitos in Aðaldalur, it matches our observations from the field. However, the spacing between the hornitos does change between the groups: those towards the end of the YLL (H2) are more widely spaced than those further up the valley (H1).

Hornitos are the smallest rootless features in Aðaldalur and show very little variation in size across the valley (Fig. S19). The two groups measured (H1 and H2) have almost identical size distributions and though this represents only a small sample of the hornitos in Aðaldalur, it matches our observations from the field. However, the spacing between the hornitos does change between the groups: those towards the end of the YLL (H2) are more widely spaced than those further up the valley (H1).

5. Discussion

The variation in types and sizes of rootless cones along the Younger Laxá Lava (YLL), from large multi-cratered scoriaceous cones to small spatter-rich hornitos, shows that there were considerable changes in the lava–water interaction (LWI) dynamics. Here, we explore how these changes relate to the environment in which the rootless cones formed, particularly the availability of lava and water. Our goal is to assess how the YLL was emplaced, what sources of water it encountered,

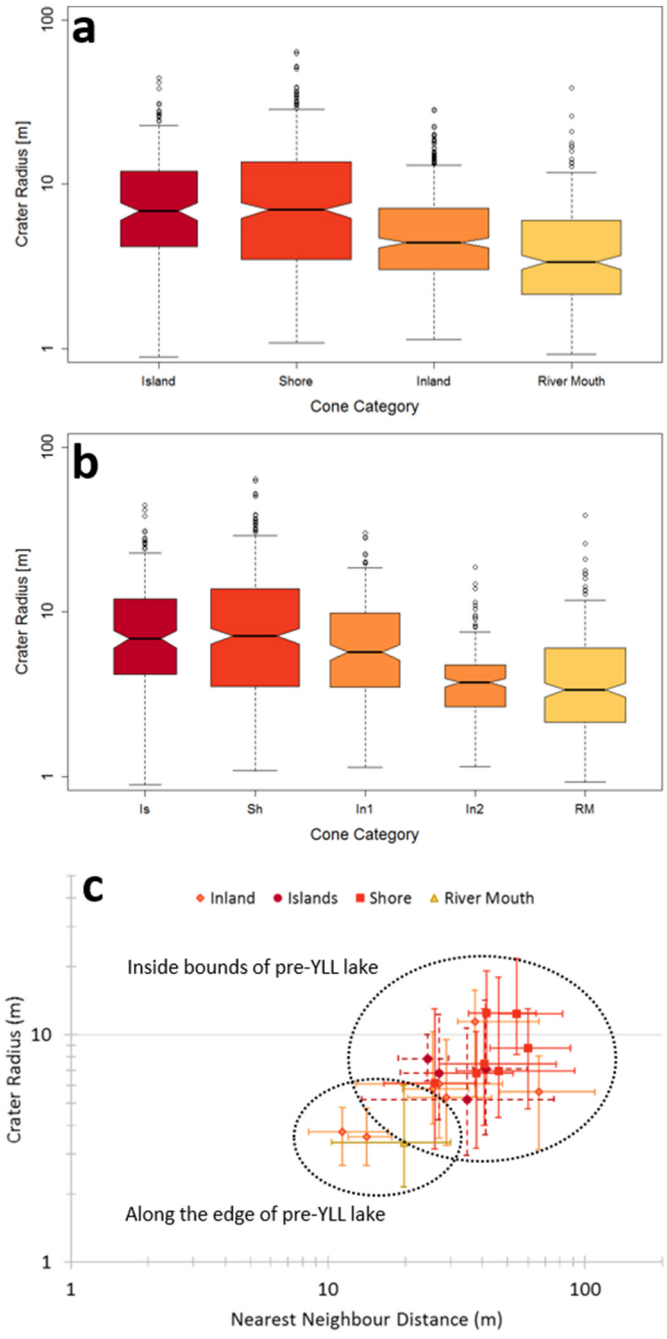

Fig. 8. Variation in crater size and spacing for Mývatn rootless cones, grouped by proximity to the lake shore lake (i.e. island, shore, inland or river mouth). **a)** Groups based on the proximity to the present-day lake. **b)** Modified groupings, with the inland cones split into those thought to be inside the bounds of the original lake (In1) and those thought to have been formed on the lake shore (In2). Box width is proportional to the number of cones in the group. **c)** Relationship between crater size and nearest neighbour distance for rootless cones at Mývatn. Each data point represents the median of a group of cones, and the error bars show the 1st and 3rd quartiles of that group. Data points are coloured by the proximity of the group to the current lake.

how it affected these water sources, and finally how changes in lava flow and water availability affected the LWI dynamics and rootless cones formations.

The landscape and environment of the region today, along with studies of the area's post-glacial history, give an insight into the likely availability of water at the time of the eruption. We use the morphology and surface features of the YLL to assess flow development as it progressed from the eruptive vent, around lake Mývatn and through both the narrow Laxárdalur and wide Aðaldalur valleys. This provides context for our statistical assessments of cone size, type, location and LWI dynamics.

Table 4
Expected and observed distributions of different types of rootless cones across the YLL based on X^2 distribution modelling.

	Mývatn		Laxádalur		Aðaldalur	
	Expected	Observed	Expected	Observed	Expected	Observed
Lotus	13.01	50	0.96	0	43.95	8
Double	22.56	97	1.66	0	75.78	3
Single	441.20	870	32.51	89	1482.29	997
Spatter	47.37	151	3.49	0	159.14	59
Pit	57.07	253	4.20	0	191.73	0
Hornito	881.95	0	65.00	0	2963.07	3910
Unclassified	29.77	72	2.19	21	100.03	39
Total		**1493**		**110**		**5016**

5.1. What does the morphology of the YLL tell us about how it was emplaced?

Surface textures and features on the YLL show that the emplacement style varied substantially between the source vent near lake Mývatn and the flow terminus in Aðaldalur. We use these changes to examine how the lava flow responded to the environment.

Lake Mývatn is close to the eruptive fissure, which supplied abundant lava from east the lake, as indicated by the broad flow lobes, lava channels and ponding at Dimmuborgir. The lava pillars, bathtub rings and other drainage features around Höfði show that the lava also ponded in this region. The extent of the YLL around the lake and the accompanying tephra blanket provide additional evidence for a high lava flux.

In Laxárdalur, much of the YLL surface has been obscured or eroded by the Laxá river, which has now reclaimed the gorge. However, the inferred 10 °C temperature drop over the 45 km (Fig. S14) shows that the flow must have formed an insulating lava tube through the valley. The narrow width of the Laxádalur gorge (0.5–1 km) would have aided tube formation and efficient transport of lava to Aðaldalur.

The variety of surface morphologies on the YLL in Aðaldalur shows that the emplacement style changed as the flow progressed. The pressure ridges and flow lobes in the upper part of the valley imply that it was emplaced as a broad sheet, with a mass flow rate low enough to form a stable top crust but high enough to deform the crust as the lava advanced (Walker, 1971; Fink and Griffiths, 1992; Kerr et al., 2006). In contrast, the numerous pits on the flow surface further down the valley indicate inflation, possibly because of a reduction in flow advance rate because of the decreasing slope of the valley floor (e.g. Hon et al., 1994). The inflation pits must have formed as the lava diverted around obstacles in its path (Hon et al., 1994; Self et al., 1998). We propose that these pits were formed where a slowly-advancing lava front was quenched by pools of water, causing the flow to divert and inflate around the pool (Fig. 10). Contact with the lava could cause the water to boil away, in which case the pool may be filled in by the advancing lava flow. However, a pit would still remain because of the inflation on either side of the pool. Some of larger pits are >9 m deep and still hold water, suggesting that they were not filled in with lava and the flow diverted around them. The rootless cones around these pits may be the result of faster-moving parts of the lava flow filling in pools and driving rootless eruptions from the saturated sediments underneath (group C cones).

The 3–6 m high step in the YLL (Fig. 6c) appears to be an inflation front, where the flow temporarily stopped advancing. The numerous rootless cones along the inflation front indicate an abundant source of water, probably from saturated underlying sediment (wetlands). Rootless eruptions along the flow front would have acted as a barrier to the lava flow, causing it to stall and inflate. Similarly, an increase in

Table 5
Rootless cone crater radius distributions by type (all dimensions in metres).

	Min	Q1	Median	Mean	Q3	Max	Std. dev.	Mean + 12.3%	Mean − 14.1%
Lotus	4.85	13.51	20.34	22.28	28.52	64.38	12.47	25.02	19.1
Double	2.60	10.07	14.34	17.41	21.66	62.34	11.13	19.55	15.0
Single	0.78	3.08	4.70	6.18	7.62	41.59	4.73	6.97	5.30
Spatter	0.87	2.39	3.68	4.57	5.67	17.16	3.02	5.13	3.93
Pit	0.89	1.72	2.42	3.28	4.01	15.96	2.39	3.63	2.82
Hornito	0.23	0.48	0.64	0.79	1.01	3.00	0.44	0.89	0.68
Unclassified	1.14	2.44	3.39	4.66	5.22	19.35	3.63	5.23	4.00

substrate saturation would increase cooling to the base of the flow, which could also cause it to stall and inflate.

5.2. What does the environment today tell us about water availability?

Einarsson (1982) showed that a larger and deeper lake existed at Mývatn before it was inundated by the YLL. He found that the lake bed was thickly coated with diatomaceous sediments, similar to those present in the lake today. Because diatoms have hollow silicate shells filled predominantly with water, these sediments can hold a much more water than sediments limited by particle packing fraction (77–78% water, rising to 98% water in the top 60 cm; Einarsson et al., 1988). The water in these sediments would have been heated by contact with the YLL and released steam, driving rootless eruptions, as shown by the presence of sediments inside vesicles in rootless tephra (Einarsson, 1982).

The distribution of rootless cones around Mývatn allows us to reconstruct the outline of the original lake and extend Einarsson's (1982) original estimate (Fig. 3b). The ArcticDEM shows that all but one of the cone groups around the lake have the same basal elevation of 279 m (Fig. 3b), which indicates that the top surface of the YLL around Mývatn was remarkably level with constant thickness (~10 m). Given the lava thickness and the presence of lake diatoms inside vesicles in rootles cones (Einarsson, 1982), the constant basal elevation of the cones suggests that they were all formed by lava interacting with the lake and lake sediments. This implies that the lake was not only larger than present, but probably linked with the smaller lake Sandvatn to the north. A more extensive lake and adjacent wetlands than at present explains the numerous scoriaceous rootless cones along the western shore and inland towards Sandvatn.

The group of cones near Dimmuborgir (group 21) has a mean basal elevation of 303.2 m (i.e. 24 m higher than the other groups and 27 m above the current lake level) but still includes diatoms consistent with the pre-existing lake (Einarsson, 1982), showing that the lake must have extended further east than at present. The difference in basal elevation is likely because the YLL is thicker in this area. No rootless cones are visible on the surface of the YLL between Dimmuborgir and the eastern edge of Mývatn, but construction of the road to Dimmuborgir revealed rootless cones buried under lava, confirming that there was sufficient water in this region to drive rootless eruptions. Given the presence of lake-dwelling diatoms in the Dimmuborgir cones (Einarsson, 1982), the edge of the pre-existing lake may have been the barrier that caused the lava flow to pond and create Dimmuborgir in the first place, rather than a water-filled fault as suggested by Skelton et al. (2016).

When the YLL reached the southwest corner of the lake, it would have blocked the flow of water into the Laxá. Comparable damming of rivers by lava was recorded during the 1783–84 Laki fissure eruption. Rev. Jón Steingrímsson, who witnessed and recorded the eruption, described how a "*cloud of smoke and steam moved along the gorge of the river Hverfisfljót*" and that "*in some channels, the water seethed with heat*" (Kunz, 1998), prior to the river level dropping and then drying up completely. It is reasonable to assume that a similar situation occurred as the YLL first heated the water in Mývatn and then dammed the Laxá, cutting off the main source of water in the gorge and leaving behind only small ponds and feeder streams from the surrounding highlands. In fact, all four cone groups in Laxárdalur coincide with the location of one of these feeder streams, although not all streams have associated rootless cones (Fig. 4). The streams would also have built deltas of wet sediment, that could have held water and contributed to rootless cone formation.

Unlike the Laxá, the source of the Reykjadalsá was unaffected by the YLL, and provided a steady, if somewhat smaller, supply of water to the top of Aðaldalur (Figs. 5, 7a). The easiest path for the YLL to follow into Reykjadalur was along the existing river channel. Damming the river would have caused localised flooding, similar to during the Laki fissure eruption. We suggest that the lakes at the mouth of Reykjadalur are the remnants of flooding caused by the YLL damming the Reykjadalsá.

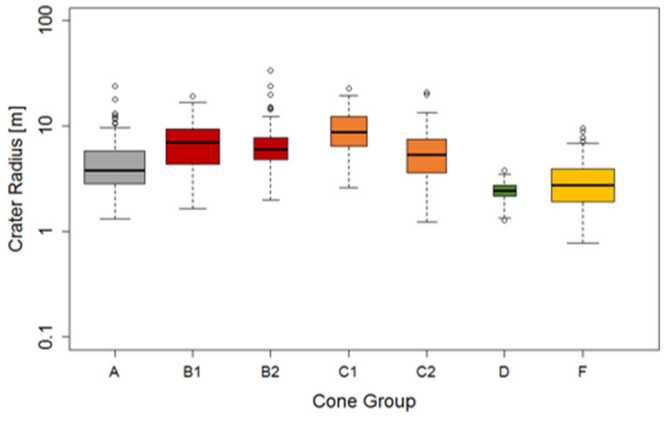

Fig. 9. Variation in single-cratered scoriaceous rootless cone crater radius for cone groups in Aðaldalur. Cones have been groups based on their location on the YLL, and group outlines are shown in Fig. 5. See Fig. S14 for size distribution of all cone types.

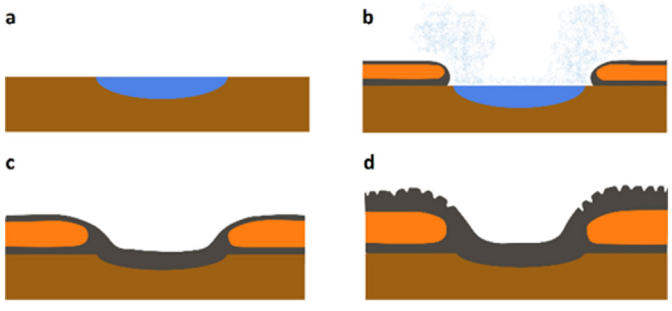

Fig. 10. Model for the formation of an inflation pits around a pool of water. **a)** Lava flow advances towards a pool of water (blue). **b)** Where the lava flow meets the water, the flow is quenched and stops advancing. The lava flow splits into lobes that flow either side of the pool. The pool is gradually boiled away or displaced by the lava flow. **c)** The lobes on either side of the pool inflate as more lava is injected and the crust thickens with cooling. The pool is gradually covered over but because the water quenched the flow around the pool, it does not inflate. Eventually all of the water in the pool is boiled away or displaced. **d)** The lobes on either side of the pool continue to advance and inflate, joining up at the far side of the pool, leaving a pit in the surface of the lava flow.

These lakes would have provided a continuous supply of water to drive rootless cones along the edge of the lava flow.

Damming the two rivers cut off the supply of water to the southern part of Aðaldalur, leaving only the water contained in pools and dispersed in sediments in wetland areas. The numerous inflation pits with standing water may be the remains of some of these ponds. At the northern end of the Fljótsheiði mountain, Aðaldalur joins the adjacent Bárðardalur valley, which hosts the braided river Skjálfandafljót (Fig. 5b). We found rounded pebbles consistent with a riverine environment embedded in a rootless cone in this part of the valley. We do not know the original position of the river, but the presence of river channels at the edge of the YLL (several hundred metres from the current path of the river; Fig. S20) suggests that it could have been a source of water for the northern part of Aðaldalur. The inflation front that lies level with the Aðaldalur–Bárðardalur valley confluence may reflect the lava flow encountering an area of increased water in the underlying sediment, most likely from a wetlands environment similar to that beyond the YLL today.

5.3. How did the changes in lava and water availability affect LWI?

From the distribution of rootless cones across the YLL and the trends in cone type and size, we can draw links between the supplies of lava and water across Mývatn, Laxárdalur and Aðaldalur and the resulting rootless eruptions. It is reasonable to assume that cone location must reflect the water availability, since rootless eruptions require water. Similarly, we can relate cone size to the supply rates of lava and water: continuous or pulsed high volume-flux supplies of lava and water will be able to sustain long-duration rootless eruptions, building up large rootless cone edifices. More limited supplies of lava or water will produce shorter eruptions and smaller cones. Since rootless cones require a stable lava flow surface to support the edifice, this implies that the lava flow is relatively well established and lava supply rate will be controlled by the thickness of the molten flow core and the internal flow velocity (we note that LWI may take place before the flow is well established but not produce surviving deposits). Pyroclast type (ash, lapilli or spatter) is controlled by the intensity of the LWI (i.e. the rate of heat transfer from lava to water and the resulting rate of steam generation).

The largest cones are found around Mývatn, which is close to the eruptive vent and provided a sufficiently large and continuous supply of water to drive long duration LWI and build large cones. While the total available volumes of lava and water do not directly control the rates of heat transfer and steam generation, the high proportion of scoriaceous (L, D, S and P) cones around Mývatn shows that there must have been intense, explosive LWIs (Fig. 7a). It is possible that the fine saturated lake sediments promoted this, and their presence inside vesicles in rootless cones suggests that they contributed to the rootless eruptions. Firstly, these sediments can retain a large volume of water (Einarsson et al., 1988) so would have increased the total available water. Secondly, their low permeability would speed the increase in pore pressure as the sediments were heated by lava. Finally, the lower density and viscosity contrasts between the lava and water-sediment mix could allow coarse mingling between the two, ultimately promoting FCI (White, 1996).

In contrast, in Aðaldalur the rootless cones are smaller, reflecting the more limited supply of water after the two rivers feeding the valley were dammed by the YLL. The shallow (~1°) slope of Aðaldalur fed by numerous rivers means that it has coarser sandy sediments and peat-like soils in wetland areas. Coarser sediments generally have higher permeability, reducing the pressure build-up as lava heats the interstitial water. In Laxárdalur, which dried up after the Laxá was dammed, sedimentary deltas from small streams probably provided water to drive rootless eruptions.

The down-flow change in to spatter features (SP and H) suggests a shift to lower energy LWI. This change occurs where we believe the available water changed from isolated pools to a wetland environment. The lack of any scoria or ash deposits at SP and hornitos implies that the conditions were not right for explosive FCI, either because there was insufficient lava or water, or because the necessary high contact area between lava and water was not achieved. These SP cones are similar in size and texture to the deposits formed by bubble bursts in littoral settings (Mattox and Mangan, 1997), suggesting a similar mechanism. Since hornitos (and spatter cones) are built by successive layers of welded spatter, their width must be controlled ballistically by the kinetic energy of steam expansion that controls the spatter trajectories, whereas their height reflects the LWI duration. This suggests that wider features form from higher energy bubble bursts, and tall features form by longer duration events (e.g. longer series of bubble bursts).

In the following sections, we illustrate specific LWI scenarios using case studies across the YLL to show how the lava flux and water availability affected the LWI dynamics and the resulting rootless cones. Examples include the change in cone size around Mývatn, the link between cone size and lava flow morphology in Aðaldalur, and the transition from scoriaceous cones to hornitos in Aðaldalur. We then briefly discuss the effect of lava and water availability on NN distribution.

5.3.1. Changes in LWI around Mývatn

Our proposed new extent of pre-YLL Mývatn (Fig. 3b) not only fits with the distribution of rootless cones around the lake, but also explains the observed variation in cone size. The inferred extent of the pre-YLL lake means that all of the rootless cones on the islands (Is), lake shore (Sh) and most of the inland groups (those categorised as In-1) would have formed within the lake and adjacent wetlands, which would have supplied these rootless eruption sites with a large and effectively continuous supply of lake water, and a high volumetric flux of lava from the nearby eruptive vent. This explains both the presence of large scoriaceous cones and the statistical similarity in size between these three cone groups (Fig. 8). In contrast, the rootless cone groups that lie near the proposed edge of the lake and along the margins of the YLL (groups 17 and 18) would have had a lower supply of both lava and water. They are predominantly S cones (Fig. S18), and their small size compared to the other Mývatn cones suggests shorter duration LWI, fitting with the reduced supplies of lava and water.

The high proportion of SP cones at the river mouth (group 20; Fig. S18) suggests lower intensity LWI. Comparing these cones with those nearby (group 20), we can see a marked transition in cone type: all of the cones in the interior of the lake are scoriaceous, with a high proportion of L and D cones, whereas those along the edges and the Laxá river channel are predominantly SP cones (Fig. 3a). The reduction in intensity may reflect the reduced supply of water as the lava dammed the Laxá.

There is also evidence for passive (non-explosive) LWI around Mývatn, in the form of lava pillars at the south-east corner of the lake. Bathtub rings indicate that the lava ponded here and then drained in stages similar to Dimmuborgir (Fig. S9c). The lava pillars resemble those described by Gregg and Christle (2013) and Skelton et al. (2016), interpreted to have formed by steam escaping passively through ponded lava, freezing the surrounding lava (Fig. S9b). The pillars at Mývatn may have been formed by the eastern edge of the lake or by feeder springs (Fig. 3b); a steady supply of water from springs under deep, ponded lava may have been enough to establish permanent outlets for steam through the lava, preventing the steam pressure from building up to explosive levels.

The buried cones on the road towards Dimmuborgir show that the scarcity of rootless cones along the eastern shore of the lake is not because there was no LWI, but because any rootless cones formed were buried by later lava flows. Buried rootless cones are also found in the Columbia River Flood Basalts (Reynolds et al., 2015). These examples suggest that rootless eruptions are more common than surviving deposits suggest.

5.3.2. Aðaldalur: The effect of local water and lava availability

The range of cone sizes and types across Aðaldalur show that the LWI dynamics varied throughout the valley. By looking at the different groups in detail, their position on the lava flow and the sources of environmental water, we can infer the effect of lava and water availability on rootless eruptions.

In the main part of Aðaldalur, rootless cone size varies with position on the lava flow. S cones make up the vast majority (98.9%) of the scoriaceous cones in this region, so to simplify the statistical modelling we consider only S cones. Cones that formed in the middle of the YLL, both on ropy and inflated pāhoehoe, are, on average, 2–3 times larger than those formed at the edge of the flow and along the inflation front (Fig. 9). This difference could reflect changes in the local lava mass flow rate, the availability of water, or both.

The location of group B1 in a topographic depression and the close NN spacing suggests that here the YLL flowed into a low-lying area of the valley with a contained supply of water. The dashed white line in Fig. S15 shows the outline of water present today, which may be the remnants of a small lake. We propose that the YLL overwhelmed this lake and that water trapped in the basin and sediment drove intense rootless eruptions (group B1.1). The smaller cones in the rest of B1 were formed by more distributed water in a wetland-type environment around the central lake. The ropy, sheet-flow morphology of the YLL in this area suggests there was a continuous supply of lava, implying that the LWI was not lava-limited. Therefore, the size of the rootless cones was probably controlled by the limited availability of water in the lake and sediment.

The largest rootless cones in Aðaldalur formed on the inflated region of the YLL (Fig. 9). The inflated flow morphology shows that the bulk advection rate of the lava flow had slowed. This slower emplacement would allow the lava front to be quenched and diverted by small pools of water, further slowing its advance and creating numerous inflation pits (Fig. 10). The diversion of flow around pools would have concentrated the lava into lobes, rather than a broad sheet, although there are no sinuous ridges or tumuli to indicate a long-lived tube system. The rootless cones do not fall into well-defined groups (C1 and C2 in Fig. 5b), but the numbers of both inflation pits and cones suggest that there was plenty of standing water, probably from wetlands and scattered pools. The similarity in cone size and types between the ropy (groups B1 and B2) and inflated (groups C1 and C2) regions suggests that the dynamics of the LWI were not significantly affected by the concentration of lava into lobes, which could have compensated for the reduced bulk flow rate (Fig. 9). The rootless cones in this region probably formed on pockets of water that were too small to quench the lava but sufficiently large to fuel rootless eruptions.

In contrast, rootless cones on the western margin of Aðaldalur and along the inflation front (groups D and F) are significantly smaller than those in the middle the YLL (Fig. 9). This could record a reduction in either the local lava mass flow rate, or the availability of water, or both. Group D cones record the presence of some water along the western edge of Aðaldalur, most likely the remains of the Reykjadalsá after it was dammed by the YLL. However, the sparseness and small size of these cones, as well as their position along the edge of the lava flow, suggest that neither water nor lava was plentiful. Therefore, we cannot separate the effects of water and lava on cone size for this group.

The hundreds of small rootless cones along the inflation front, in contrast, suggest a plentiful and widely distributed source of water in the area, probably distributed in the underlying sediment rather than contained within discrete pools, and an evenly distributed supply of lava along the inflation front. We suggest that this combination of a lower, more distributed supply of both lava and water drove numerous, short-lived rootless eruptions along the inflation front, creating the smaller, more closely spaced rootless cones in this region.

In summary, although we cannot completely distinguish the individual effects of lava and water availability on LWI, placing the trends in cone size and spacing found in our statistical analysis in the context of the lava flow morphology and available water helps interpret the variation in the deposits.

5.3.3. The change from scoriaceous cones to hornitos

The trends discussed above relate to the variation in S cones, but the lower part of Aðaldalur is covered almost exclusively in hornitos. The abrupt change from predominantly scoriaceous cones to hornitos marks a step-change in the dynamics of LWI in the valley and coincides with the position of the YLL inflation front. Moreover, almost all of the SP cones in Aðaldalur are found along this boundary (Fig. 6c). Their location and intermediate size between small S cones and hornitos suggests that SP cones are transitional features, produced as the rootless eruptions changed from explosions capable of producing ash and scoria to milder eruptions, generating only spatter. The stalling of the lava flow and the concentration of rootless cones along the inflation front suggest the presence of widespread water at or near the surface (i.e. an increase in saturation and/or permeability of the underlying sediment). Therefore, it is likely that the shift in LWI style that formed the hornitos is also linked to this change.

The hornitos in Aðaldalur are widespread, covering an estimated 2.5 km^2. UAS surveys near the inflation front and at the far end of the YLL, and broader field observations, indicate that there is very little variation in hornito size across the valley. The two sample groups (H1, H2) are statistically indistinguishable and have the lowest variation in crater size of any rootless cone type (Fig. S19). This lack of variation implies that there was little change in either the supply of lava or availability of water across this part of the flow. Hornitos on top of lava tubes are formed by low energy degassing and spattering, and it is likely that the hornitos in Aðaldalur were formed in a similar way. In the case of Aðaldalur hornitos, however, the driving force was steam escaping from a widely distributed water source under the lava flow, probably underlying saturated sediments. Another lava flow with large numbers of hornitos is in the Wudalianchi National Park in China, where lava flowed over a shallow lake (Gao et al., 2013).

The change in dynamics of the LWI from explosive to bubble-burst eruptions, and the implied reduction in LWI intensity, suggests that the rate of heat transfer between lava and water, and therefore the rate of steam generation, decreased significantly beyond the inflation front. We cannot be certain why the intensity dropped, but we suggest three factors that would have a strong influence. Firstly, the widespread formation of hornitos required a widely distributed water source, most likely saturated sediment. Where lava interacts with contained water (e.g. a lake or pool), most of heat transferred from the lava will generate steam. The presence of sediment, however, would act as a contaminant that reduces the heat transfer rate between the lava and water by absorbing some of the heat itself (White, 1996). Secondly, hornitos are >50 km from the eruptive fissure. On its journey through Laxárdalur, the YLL was well insulated by a lava tube formed in a narrow valley. However, as the lava spread out across Aðaldalur, the surface area to volume ratio increased, increasing the cooling rate of the lava. This is reflected in the change in flow morphology from an insulated tube to a broad sheet flow and then to an inflated flow. Thirdly, the type of sediment in the valley may have contributed to hornito formation. Wetland environments in Iceland today have peaty soils that hold lower volumes of water than lake sediments. Peaty soils would not readily mingle with lava, hindering FCI. However, if the YLL caused an underlying peat bog to burn, it would release CO_2 and methane. Because peat burns slowly, these volatiles would build up until they could overcome the confining pressure of the lava flow as bubble bursts and building up hornitos. The lava flow is a few metres thinner downstream of the inflation front, indicating a diminished lava supply and therefore lower confining pressure on the underlying sediment. The low energy release of these hot gasses may have generated spatter and contributed to hornito formation. It is possible that the combination of a lower supply rate, cooler lava and slow rates of water release would lead to passive volatile

escape through the YLL in bubble-bursts, creating spatter cones and hornitos instead of scoriaceous rootless cones.

5.3.4. The relationship between cone size and spacing

The analysis and discussion so far has considered rootless cones forming in isolation, but many cones form in close proximity to their neighbours, often overlapping. This raises the possibility of adjacent cones interacting with one another during formation. The correlation between crater size and NN distance suggests that cone spacing is also controlled by the supply of water and lava to the rootless eruption sites (Fig. 7b).

We use the heuristic model that adjacent rootless cones compete for a limited supply of water (Hamilton et al., 2010b) to consider the effect of NN interaction on cone size. In this model, the size of an active rootless cone would be limited by the proximity of its neighbours, which would 'compete' for resources (i.e. lava and water). If active cones are close together, there will be less water and lava available for each rootless eruption site, limiting the duration of the LWI, and therefore cone size. This explains the correlation between cone size and NN distance found in this study for all cones except hornitos.

Hornitos have the lowest size variability of any type of rootless cone, and their size does not correlate with NN distance. This fits with our suggestion that the dynamics of LWI creating hornitos are substantially different to other rootless cones. Hornitos sit at the lowest energy end of the LWI spectrum, formed by spattering more akin to bubble bursts than explosions. The low energy of this interaction is more likely to limit their size than competition from nearby hornitos.

6. Summary

The YLL and its associated rootless cones provide an excellent case study for understanding the dynamics of LWI during lava flow emplacement. Comparing the rootless cones in Mývatn, Laxárdalur and Aðaldalur shows the effect of the supply of water and lava on the type and size of the cones formed. The cone distribution around Mývatn reveals the extent of the pre-existing lake, showing how it was modified by the YLL. Rootless cones size is related to their proximity to the original lake, with larger cones found nearer the middle of the lake, and smaller cones around the edges, reflecting the availability of water. Damming of the river Laxá at the outlet from Mývatn explains the relative scarcity and small size of cones in Laxárdalur, as well as their location where smaller streams and channels drain the surrounding hills. Laxárdalur's narrow aspect, together with upstream damming, permitted thermally efficient transport of lava through the valley, probably via an insulating lava tube. The different cone groups in Aðaldalur reflect the different water sources that the YLL encountered and how it interacted with them: damming and flooding a river flowing in from the adjacent valley, inundating small lakes and pools, or bypassing and inflating around them. The smaller rootless cones found along the edges of the lava flow and along the inflation front demonstrate the effect of a lower local mass flow rate of lava compared to the middle of the lava flow. The abrupt change from scoriaceous cones to spatter cones and hornitos in Aðaldalur, coincident with a preserved inflation front, suggests a change in LWI dynamic, probably a response to the substrate changing to a wetland environment with abundant water distributed throughout the sediment rather than in discrete pools. Stalling and inflation of the YLL reflect this change in substrate; water-logged sediment would increase the cooling at the base of the flow and drive the formation of rootless cones seen all along the inflation front.

From our observations, we predict the types rootless cones that would be expected for given lava and water supplies. Environments with abundant water and lava (e.g. a large lake close to the eruptive vent) create larger rootless cones and a higher proportion of multicratered cones. In contrast, areas where there is less available water, such as (temporarily dammed) river valleys, smaller lakes or wetlands, produce fewer and smaller rootless cones. Similarly, rootless cones along inflation fronts and the edges of lava flows are smaller because of the reduced local mass flow rate of lava. The size of the rootless cones also correlates with the distance to their NN and may be the result of adjacent cones 'competing' for finite amounts water and lava, reducing the duration of the LWI and limiting the size of the resulting cones. The spacing of the cones will also depend on the distribution of water: concentrated and plentiful water supplies will produce discrete clusters rather than widely distributed rootless cones. With decreasing intensity of LWI comes a change in rootless eruption dynamics, from cones of scoria and ash to spatter cones and hornitos suggestive of littoral bubble bursts (Mattox and Mangan, 1997). At the lowest energy end of the LWI spectrum, large fields of hornitos can be created, most likely as a result of steam escaping through a lava flow from a saturated substrate.

Using case studies like the YLL to link rootless cone type and size to lava supply and water availability gives us insight into how these factors affect rootless eruption dynamics. Understanding the type of cones likely to form in different conditions can inform hazard assessments for future lava flows interacting with water and helps us interpret existing deposits on Earth and Mars.

Supplementary data to this article can be found online at https://doi.org/10.1016/j.jvolgeores.2018.08.019 and in the University of Brisol data repository at https://data.bris.ac.uk/data/dataset/ojcw17r060lu21o7lbjeoftbf.

Acknowledgements

The authors would like to thank Dr. Tom Richardson of the University of Bristol for the loan of the UAS used for this work. We would also like to thank Jennifer Saxby for her help in the field, and Isabel Wilson and Bob Myhill for their guidance on statistical modelling. We thank Hannah Buckland for her help collecting glass chemistry from the thin section samples. We also thank Christopher Hamilton and one anonymous reviewer for their thorough and constructive comments on this paper. This work was supported by the Natural Environmental Research Council [grant no: NE/L002434/1], and on AXA Research Fund and Wolfson Merit Award to KVC. DTMs provided by the Polar Geospatial Center under NSF OPP awards 1043681, 1559691 and 1542736.

References

Aebischer, J., 2018. Syneruptive crystallisation and degassing in the Laxárhraun lava flow, Northern Iceland. MSc Thesis. ETH Zurich.

Austin-Erickson, A., Büttner, R., Dellino, P., Ort, M.H., Zimanowski, B., 2008. Phreatomagmatic explosions of rhyolotic magma: Experimental and field evidence. J. Geophys. Res. 113. https://doi.org/10.1029/2008JB005731.

Cashman, K.V., Mangan, M.T., 2014. A century of studying effusive eruptions in Hawai'i. In: Poland, M.P., Takahashi, T.J., Landowski, C.M. (Eds.), Characteristics of Hawaiian Volcanoes. vol. 1801. USGS Professional Paper.

Cummins, A., 2017. BBC Crew Makes Dramatic Escape as Mount Etna Volcano Erupts. CNN 17 March 2017. https://edition.cnn.com/2017/03/17/europe/bbc-crew-volcano-mount-etna-eruption/index.html, Accessed date: 1 August 2018.

Edwards, B., Magnússon, E., Thordarson, T., Guðmundsson, M., Höskuldsson, A., Oddson, B., Haklar, J., 2012. Interactions between lava and snow/ice during the 2010 Fimmvörðuháls eruption, south-central Iceland. J. Geophys. Res. 117 (B4). https://doi.org/10.1029/2011JB008985.

Einarsson, Á., 1982. The palaeolimnology of Lake Mývatn, northern Iceland: plant and animal microfossils in the sediment. Freshw. Biol. 12, 63–82.

Einarsson, Á., Halfliðalson, H., Óskarsson, H., 1988. Mývatn: Saga lífríkis og gjóskutímatal í Syðriflóa. Rannsóknastöð við Mývatn. Skýrsla 4, Reykjavik.

Einarsson, Á., Stefánsdóttir, G., Jóhannesson, H., Ólafsson, J., Gíslason, G., Wakana, I., Gudbersson, G., Gardarsson, A., 2004. The ecology of Lake Mývatn and the River Laxá: variation in space and time. Aquat. Ecol. 38, 317–348.

Fagents, S., Thordarson, T., 2007. Rootless volcanic cones in Iceland and on Mars. In: Chapman, M.G. (Ed.), The Geology of Mars: Evidence from Earth-based Analogs. Cambridge University Press, Cambridge, pp. 151–177.

Fagents, S., Lanagan, P., Greeley, R., 2002. Rootless cones on Mars: a consequence of lava-ground ice interaction. In: Smellie, J.L., Chapman, M.G. (Eds.), Volcano-Ice Interaction on Earth and Mars. vol. 202. Geol. Soc. Lond. Spec. Pub., pp. 295–317.

Fink, J.H., Griffiths, R.W., 1992. A laboratory analog study of the surface morphology of lava flows extruded from point and line sources. J. Volcanol. Geotherm. Res. 54, 19–32.

Fisher, R.V., 1968. Pu'u Hou littoral cones, Hawaii. Geol. Rundsch. 57, 837–864.

Fitch, E.P., Fagents, S.A., Thordarson, T., Hamilton, C.W., 2017. Fragmentation mechanisms associated with explosive lava–water interactions in a lacustrine environment. Bull. Volcanol. 79 (12).
Gao, W., Li, J., Mao, X., Li, H., 2013. Geological and Geomorphological Value of the Monogenetic Volcanoes in Wudalianchi National Park, NE China. Geoheritage 5, 73–85.
Greeley, R., Fagents, S.A., 2001. Icelandic pseudocraters as analogs to come volcanic cones on Mars. J. Geophys. Res. 106, 20,527–20,546.
Gregg, T.K.P., Christle, K.W., 2013. Non-explosive lava–water interaction in Skaelingar, Iceland and the formation of subaerial lava pillars. J. Volcanol. Geotherm. Res. 264, 36–48. https://doi.org/10.1016/j.jvolgeores.2013.07.006.
Gregg, T.P.K., Fornari, D.J., Perfitt, M.R., Ridley, W.I., Kurz, M.D., 2000. Using submarine lava pillars to record mid-ocean ridge eruption dynamics. Earth Planet. Sci. Lett. 178, 195_214. https://doi.org/10.1016/S0012-821X(00)00085-6.
Hamilton, C.W., Thordarson, Th., Fagents, S.A., 2010a. Explosive lava–water interactions I: architecture and emplacement chronology of volcanic rootless cone groups in the 1783-1784 Laki lava flow, Iceland. Bull. Volcanol. 72, 449–467.
Hamilton, C.W., Fagents, S.A., Thordarson, Th., 2010b. Explosive lava–water interactions II: self-organization processes among volcanic rootless eruption sites in the 1783–1784 Laki lava flow, Iceland. Bull. Volcanol. 72, 469–485.
Hamilton, C.W., Fagents, S.A., Thordarson, Th., 2011. Lava-ground ice interaction in Elysium Planitia, Mars: Geomorphological and geospatial analysis of the Tartarus Colles cone groups. J. Geophys. Res. 116, E03004.
Hamilton, C.W., Fitch, E.P., Fagents, S.A., Thordarson, Th., 2017. Rootless tephra stratigraphy and emplacement processes. Bull. Volcanol. 79, 11.
Hauptfleisch, U., Einarsson, Á., 2012. Age of the Younger Laxá Lava and Lake Mývatn, Northern Iceland, determined by AMS radiocarbon dating. Radiocarbon 54, 155–164.
Hon, K., Kauahikaua, J., Denlinger, R., MacKay, K., 1994. Emplacement and inflation of pāhoehoe sheet flows: Observations and measurements of active lava flows on Kilauea Volcano, Hawaii. Geol. Soc. Am. Bull. 106, 351–370. https://doi.org/10.1130/0016-7606(1994)106<0351:EAIOPS>2.3.CO;2.
Höskuldsson, Á., Dyrh, C., Dolvik, T., 2010. Grænavatnsbruni og Laxárhraun yngra. Fall Meeting JFI 2010, Ágrip erinda Jaðfræðafélag Íslands, 65 bls.
Jaeger, W.L., Keszthelyi, L.P., Skinner, J.A., Milazzo, M.P., McEwen, A.S., Titus, T.N., Rosiek, M.R., Galuszka, D.M., Howington-Kraus, E., Kirk, R.L., 2015. HiRISE Team (2010) Emplacement of the youngest flood lava on Mars: A short, turbulent story. Icarus 230–243.
Jakobsson, Þ., 1963. Myndun Aðaldals. Árbók Þingeyinga 112–122.
Jurado-Chichay, Z., Rowland, S., Walker, G.P.L., 1996. The formation of circular littoral cones from tube-fed pāhoehoe: Mauna Loa, Hawai'i. Bull. Volcanol. 57, 471–482. https://doi.org/10.1007/BF00304433.
Kauahikaua, J., Sherrod, D.R., Cashman, K.V., Heliker, C., Hon, K., Mattox, T., Johnson, J., 2003. Hawaiian lava-flow dynamics during the Pu'u 'Ō'ō-Kūpaianaha eruption: a tale of two decades. US Geol. Surv. Prof. Pap. 1676, 63–87.
Kerr, R.C., Griffiths, R.W., Cashman, K.V., 2006. Formation of channelized lava flows on an unconfined slope. J. Geophys. Res. Solid Earth 111 (B10). https://doi.org/10.1029/2005JB004225.
Keszthelyi, L.P., Jaeger, W.L., Dundas, C.M., Martínez-Alonso, S., McEwen, A.S., Milazzo, M.P., 2010. Hydrovolcanic features on Mars: preliminary observations from the first Mars year of HiRISE imaging. Icarus 205, 211–229.
Kunz K (Trans.), 1998. In: Th, Skúladóttir (Ed.), Fires of the Earth: The Laki Eruption 1783–1784 by the Rev. Jón Steingrímsson. University of Iceland Press, Reykjavik.
Liu, E.J., Cashman, K.V., Rust, A.C., Gislason, S.R., 2015. The role of bubbles in generating fine ash during hyromagmatic eruptions. Geology 43, 239–242 (doi: 10.1130'G36336.1).
Liu, E.J., Cashman, K.V., Rust, A.C., Höskuldsson, A., 2017. Contrasting mechanisms of magma fragmentation during coeval magmatic and hydromagmatic activity: the Hverfjall Fires fissure eruption, Iceland. Bull. Volcanol. 79, 68. https://doi.org/10.1007/s00445-017-1150-8.
Mattox, T.N., 1993. When lava meets the sea: Kilauea Volcano, Hawai'i. Earthquake Volcanol. 24 (4), 160–177.
Mattox, T.N., Mangan, M.T., 1997. Littoral hydrovolcanic explosions: a case study of lava-seawater interaction at Kilauea Volcano. J. Volcanol. Geotherm. Res. 75, 1–17. https://doi.org/10.1016/S0377-0273(96)00048-0.
Mattsson, H.B., Höskuldsson, Á., 2011. Contemporaneous phreatomagmatic and effusive activity along the Hverfjall eruptive fissure, north Iceland: Eruption chronology and resulting deposits. J. Volcanol. Geotherm. Res. 201, 241–252.
Moore, J.G., Ault, W.U., 1965. Historic littoral cones in Hawaii. Pac. Sci. 19, 3–11.
Noguchi, R., Kurita, K., 2015. Unique characteristics of cones in Central Elysium Planitia. Mars, Planetary and Space Science 111, 44–54.
Noguchi, R., Höskuldsson, Á., Kurita, K., 2016. Detailed topographical, distributional, and material analyses of rootless cones in Myvatn, Iceland. J. Volcanol. Geotherm. Res. 318, 89–102.
Noh, M.-J., Howat, I.M., 2015. Automated stereo-photogrammetric DEM generation at high latitudes: Surface Extraction with TIN-based Search-space Minimization (SETSM) validation and demonstration over glaciated regions. GIScience & Remote Sensing 52, 198_217. https://doi.org/10.1080/15481603.2015.1008621.
Pedersen, G.B.M., Höskuldsson, A., Dürig, T., Thordarson, T., Jónsdottir, I., Riihuus, M.S., Óskarsson, B.V., Dumont, S., Magnusson, E., Gudmundsson, M.T., Sigmundsson, F., Drouin, V.J.P.B., Gallagher, C., Askew, R., Gudnason, J., Moreland, W.M., Nikkola, P., Reynolds, H.I., Schmith, J., 2017. Lava field evolution and emplacement dynamics of the 2014–2015 basaltic fissure eruption at Holuhraun, Iceland. J. Volcanol. Geotherm. Res. 340, 155–169.
Putirka, K., 2008. Thermometers and barometers for volcanic systems. Rev. Mineral. Geochem. 69, 61–120. https://doi.org/10.2138/rmg.2008.69.3.
Reynolds, P., Brown, R.J., Thordarson, T., Llewellin, E.W., Fielding, K., 2015. Rootless cone eruption processes informed by dissected tephra deposits and conduits. Bull. Volcanol. 77 (9), 72. https://doi.org/10.1007/s00445-015-0958-3.
Ross, K.A., Smets, B., De Batist, M., Hilbe, M., Schmid, M., Anselmetti, F.S., 2014. Lake-level rise in the late Pleistocene and active subaquatic volcanism since the Holocene in Lake Kivu, East African Rift. Geomorphology 221, 274–285.
Sæmundsson, K., Hjartarson, Á., Kadal, I., Sigurgeirsson, M.Á., Kristinsson, S.G., Víkingsson, S., 2012. Geological Map of the Northern Volcanic Zone, Iceland. Norther Part 1: 100,000. Iceland GeoSurvey and Landsvirkjun, Reykjavik.
Self, S., Keszthelyi, L., Thordarson, Th., 1998. The Importance of Pāhoehoe. Annu. Rev. Earth Planet. Sci. 26, 81–110.
Sheridan, M.F., Wohletz, K.H., 1983. Hydrovolcanism: Basic Considerations and Review. J. Volcanol. Geotherm. Res. 17, 1–29.
Skelton, A., Sturkell, E., Jokobsson, M., Einarsson, D., Tollefsen, E., Orr, T., 2016. Dimmuborgir: a rootless shield complex in northern Iceland. Bull. Volcanol. 78 (40). https://doi.org/10.1007/s00445-016-1032-5.
Stevenson JA, Mitchell NC, Mochrie F, Cassidy M, Pinkerton H (2012) Lava penetrating water: the different behaviours of pāhoehoe and 'a'ā at the Nesjahraun, Þingvellir, Iceland, Bull. Volcanol. 74:33–46
Sumner, J.M., Black, S., Matela, R.J., Wolff, J.A., 2005. Spatter. J. Volcanol. Geotherm. Res. 142, 49–65.
Thorarinsson, S., 1951. Laxárgljúfur and Laxárhraun: A tephrochonological study. Geogr. Ann. 33, 1–89.
Thorarinsson, S., 1953. The Crater Groups in Iceland. Bull. Volcanol. 14, 3–44.
Thorarinsson, S., 1979. The Postglacial history of the Mývatn area. Oikos 32, 17–28.
Walker, G.P.L., 1971. Compound and simple lava flows and flood basalts. Bull. Volcanol. 35, 579–590.
Walker, G.P.L., Croasdale, R., 1971. Characteristics of some basaltic pyroclasts. Bull. Volcanol. 35, 303–317.
White, J.D.L., 1996. Impure coolants and interaction dynamics of phreatomagmatic eruptions. J. Volcanol. Geotherm. Res. 74, 155–170.
White, J.D.L., Valentine, G.A., 2016. Magmatic versus phreatomagmatic fragmentation: Absence of evidence is not evidence of absence. Geosphere 12 (5), 1478–1488 (doi: https://doi.org/10.1130/GES01337.1).
Wohletz, K., Zimanowski, B., Büttner, R., 2013. In: Fagents, S.A., TKP, Gregg, RMC, Lopes (Eds.), Magma–Water Interactions in Modeling Volcanic Processes: The Physics and Mathematics of Volcanism. Cambridge University Press, Cambridge UK.
Zimanowski, B., Büttner, R., Lorenz, V., Häfele, H.-G., 1997a. Fragmentation of basaltic melt in the course of explosive volcanism. J. Geophys. Res. 102, 803–814.
Zimanowski, B., Büttner, R., Lorenz, V., 1997b. Premixing of magma and water in MFCI experiments. Bull. Volcanol. 58, 491–495.